2017

The Effect of Gram-Positive Staphylococcus Aureus Cell Wall Components Lipoteichoic Acid and Peptidoglycan on Cytokine Production, Cytoskeletal Arrangement, and Cell Viability on RAW 264.7 Murine Macrophages

Gabrielle String
Wright State University

THE EFFECT OF GRAM-POSITIVE *STAPHYLOCOCCUS AUREUS* CELL WALL COMPONENTS LIPOTEICHOIC ACID AND PEPTIDOGLYCAN ON CYTOKINE PRODUCTION, CYTOSKELETAL ARRANGEMENT, AND CELL VIABILITY ON RAW264.7 MURINE MACROPHAGES

A thesis submitted in partial fulfillment

of the requirement for the degree of

Master of Science

By

GABRIELLE STRING

B.S., State University of New York at Oswego, 2015

2017

Wright State University

WRIGHT STATE UNIVERSITY
GRADUATE SCHOOL

July 27, 2017

I HEREBY RECOMMEND THAT THE THESIS PREPARED UNDER MY SUPERVISION BY Gabrielle String ENTITLED The Effect of Gram-Positive *Staphylococcus aureus* Cell Wall Components Lipoteichoic Acid and Peptidoglycan on Cytokine Production, Cytoskeletal Arrangement, and Cell Viability on RAW 264.7 Murine Macrophages BE ACCEPTED IN PARTIAL FULFILLMENT OF THE REQUIREMENTS FOR THE DEGREE OF Master of Science.

Nancy J. Bigley, Ph.D.
Thesis Director

Committee on Final Examination

Nancy J. Bigley, Ph.D.
Professor of Microbiology and Immunology

Barbara E. Hull, Ph.D.
Professor of Biological Sciences

Dawn P. Wooley, Ph.D.
Associate Professor of Neuroscience, Cell Biology & Physiology

Robert E.W. Fyffe, Ph.D.
Vice President of Research and Dean of Graduate School

Barbara E. Hull, Ph.D.
Director of Microbiology and Immunology Program, College of Science and Mathematics

ABSTRACT

String, Gabrielle. M.S. Microbiology and Immunology Graduate Program, Wright State University, 2017. The Effect of Gram-Positive *Staphylococcus aureus* Cell Wall Components Lipoteichoic Acid and Peptidoglycan on Cytokine production, Cytoskeletal Arrangement, and Cell Viability on RAW 264.7 Murine Macrophages.

In this study, gram positive *Staphylococcus aureus* cell wall components such as lipoteichoic acid (LTA) and peptidoglycan (PGN) were used to study the potential inflammatory and anti-inflammatory cytokine response, cytoskeletal arrangement and cell viability on RAW264.7 murine macrophages over 24 hours. The effect of *S.aureus* LTA and PGN (5 μg/mL) on RAW 264.7 macrophages was evaluated every six hours for twenty-four hours. Inflammatory cytokine (TNF-α) production peaked at 6 hours before decreasing over time. Anti-inflammatory cytokine (IL-10) production peaked between 12 and 18 hours. During the first twenty-four hours, cytotoxicity of treated macrophages, as defined as the release of lactate dehydrogenase, did not increase suggesting the drop in inflammatory cytokine production was not due to cell death. As exposure to *S.aureus* cell wall components increased over twenty-four hours, cells transformed from a circular-profile M1 phenotype to a more elongated M2 phenotype. The results of this study indicate that the inflammatory response to *S.aureus* peaks early at 6 hours before being modulated by production of anti-inflammatory IL-10 later at 12 to 18 hours.

TABLE OF CONTENTS

LIST OF FIGURES

LIST OF TABLES

LIST OF EQUATIONS

List of Abbreviations

BFA - Bredeilden A solution

BSA - Bovine serum albumin

CA - Community-associated

CARMA1 - Caspase recruitment domain-containing membrane associated guanylate kinase 1

CD – Cluster of differentiation

dADO – 2' Deoxyadenosine

DMEM – Dulbecco's modified eagle's medium

DUSP1 – Dual-specificity protein phosphatase 1

ELISA – Enzyme-linked immunosorbent assay

FBS – Fetal Bovine Serum

HA – Healthcare-associated

IKKβ – Inhibitor of nuclear Factor-κB kinase Subunit β

IL-10 – Interleukin-10

JAK – Janus kinase

LDH – Lactate dehydrogenase

LPS – Lipopolysaccharide

LTA – Lipoteichoic acid

MHC – Major histocompatibility complex

MVs – Membrane vesicles

MYD88- Myeloid differentiation primary response gene 88

NETs – Neutrophil extracellular traps

NK-κB – Nuclear factor–κB

NOD – Nucleotide-binding oligomerization domain-like receptors

PBS – Phosphate buffered saline

PGN – Peptidoglycan

RICK – Receptor-interacting serine/threonine kinase

S.aureus – *Staphylococcus aureus*

SCV – Small colony variants

STAT- Signal transducer and activator of transcription proteins

TAK-1 – Mitogen-activated protein kinase-kinase-kinase-7

TLR – Toll-like receptor

TNF-α – Tumor necrosis factor-α

ACKNOWLEDGEMENT

I would like to thank Dr. Nancy Bigley for her support and advice in the completion of my project. I would also like to thank Dr. Barbara Hull for her guidance and suggestions in the completion of my project; I would also like to thank Dr. Dawn Wooley for her advice in finishing my thesis. I greatly appreciate all of your advice and for being on my committee. A very large thank you to my friends for their support, assistance, and laughter when the stress appeared too great to handle. Lastly, I would like to thank my family for supporting my decision to continue my education and move far away from home to do so. I would not have been able to complete this thesis without the advice and support from everyone.

I. INTRODUCTION

Staphylococcus aureus (*S.aureus*) is a gram-positive opportunistic pathogenic bacterium found in nasal flora of approximately 60% of the human population. In a given individual, *S.aureus* is able to exist as part of the normal flora without causing harm to its host (Fournier and Philpott, 2005). The strain colonized in the individual neonates and becomes part of that person's normal flora (Shinefeild & Ruff, 2009). *S.aureus* is also found in skin (Shinefeild & Ruff, 2009). Unfortunately, transmission of *S.aureus* from its typical flora environment to a new environment, such as a wound or surgical site, has been known to cause severe infections, and possibly death. Originally, *S.aureus* infections were treated using β-lactam antibiotics (Naimi et al., 2005). Unfortunately, antibiotic resistance has greatly increased in *S.aureus* strains (Naimi et al., 2005). This resistance makes understanding the body's immune response to *S.aureus* infections critical to combat infections and increase awareness.

Penicillin was widely used during World-War II to prevent infections from warfield surgical sites (Ventola, 2015). Shortly following the introduction of penicillin, resistant *S.aureus* strains were discovered (Ventola, 2015). New β-lactam antibiotics were discovered, including methicillin in 1960 (Ventola, 2015). Unfortunately by 1962, the first strain of *S.aureus* to be resistant to methicillin emerged in a hospital (Ventola, 2015). Many other antibiotics, such as vancomycin and linezolid, have emerged as possible

treatments for resistant strains of *S.aureus* (Ventola, 2015). Scientists and antibiotic resistant bacteria seem to be playing a game of cat and mouse, as a new antibiotic emerges, a resistant strain emerges shortly after. The emergence of antibiotic resistance is due to antibiotic resistant plasmids, such as *Cmec*, transferring from other resistant bacteria via horizontal gene transfer (David & Daum, 2010). Recently, vancomycin resistant strains of *s.aureus* have emerged, vancomycin was previously known as the drug of last resort when it comes to treating staphylococcal infections (Ventola, 2015).

Staphylococcus aureus infections are classified in two ways: healthcare-associated (HA) or community-associated (CA) (David & Daum, 2010). CA *S.aureus* strains are classified as strains which cause infections in individuals who are not associated with the health care system, such as people who are not immunocompromised (David & Daum, 2010). HA *S.aureus* strains commonly cause infections in people who are immunocompromised, for example after surgery or in a wound care facility (David & Daum, 2010). CA strains typically infect younger individuals, while HA strains tend to infect older, immunocompromised individuals (David & Daum, 2010). Virulence of HA and CA strains differ; HA strains of *S.aureus* typically include an entire cassette of the methicillin resistance gene, whereas CA strains typically carry smaller fragments (David & Daum, 2010).

Staphylococcus aureus possesses many features to evade the immune response triggered in its host. Almost immediately following *S.aureus* infection, macrophages phagocytize the bacteria and initiate the immune responses (Foster, 2005). However, select *S.aureus* strains are resistant to phagocytosis by macrophages. Many staphylococcal anti-phagocytic factors include Protein A, Clumping Factor A, and a capsule which make phagocytosis by macrophages difficult (Foster, 2005). When phagocytosis of certain strains occurs, *S.aureus* has the ability to survive inside macrophages as Small Colony Variants (SCV) (Eiff et al., 2006). SCVs may lie dormant inside a cell, replicating slowly, and may cause chronic (Eiff et al, 2006). SCVs are capable of moving into host cells, and have caused chronic infections as well as several diseases such as osteomyelitis (Eiff et al., 2006).

S.aureus secretes chemotaxic inhibitor proteins which prevent neutrophil migration from the blood to the site of infection Foster, 2005). Approximately 60% of *S.aureus* strains secrete chemotaxis inhibitory protein. Characterized by the binding of the formyl peptide receptor and the C5a receptor, this binding is responsible for inhibiting chemotaxis (Foster, 2005). C5a is essential to the complement innate immune response (Foster, 2005). Several strains of *S.aureus* also have the ability to produce toxins which can destroy leukocytes (Foster, 2005). Cytolytic toxins have a high affinity for leukocytes. Once the toxin finds a leukocyte, it forms a β-barrel in the cytoplasmic membrane which

will eventually cause the cell to burst (Otto, 2014). Recently, the cytolytic toxins have been highly associated with CA *S.aureus* infections (Foster, 2005).

A macrophage is considered a professional phagocytic cell, meaning that the macrophage surface expresses many different receptors which will assist in recognition of pathogens (Duque and Descoteaux, 2014). The primary role of macrophages is to recognize and engulf pathogens (Duque and Descoteaux, 2014). Essentially, macrophages display three phenotypic subtypes: M0, M1, and M2 (Duque and Descoteaux, 2014). M0 macrophages are un-polarized, meaning they are not yet inflammatory or anti-inflammatory (Duque and Descoteaux, 2014). Typically, an M0 macrophage, also known as a monocyte, is found as an inactivated cell in the blood of an individual (Duque and Descoteaux, 2014). Depending upon the activating substance, a macrophage may polarize into either an M1 or an M2 phenotype. M1 macrophages are pro-inflammatory macrophages induced activation by inflammatory cytokines such as Lipopolysaccharide and Interferon-γ (Duque and Descoteaux, 2014). M2 macrophages are anti-inflammatory, induced activation by Interleukin-10, Interleukin-4, and Interleukin-13 (Duque and Descoteaux, 2014). In the body, inflammatory cytokines attract more cells to the area to help combat the infection, whereas anti-inflammatory cytokines prevent inflammation and are involved in tissue repair (Duque and Descoteaux, 2014). The balance is important to combat infection without causing further harm to the host.

In addition to tactics to evade the innate immune system, toxigenic strains of *S.aureus* poses the capability to produce superantigens. Approximately 1 to 2 weeks after infection, *S.aureus* produces superantigens that are capable of activating up to 30% of T cells to induce a massive cytokine response (Lin and Peterson, 2010). The massive cytokine response causes cell death as well as additional clinical symptoms such as fever, rash, and multi-organ failure (Lin and Peterson, 2010). The emergence of multi-antibiotic resistant *S.aureus*, highlights the importance of a vaccine to increase the innate clearance of *S.aureus* prior to the production of superantigens.

II. HYPOTHESIS

RAW264.7 murine macrophages when exposed to gram-positive *Staphylococcus aureus* cell wall components lipoteichoic acid and peptidoglycan will induce changes in cell viability, cytokine production, and cytoskeletal arrangement over twenty-four hours. I predict that as the exposure time to the *S.aureus* components increases, the anti-inflammatory cytokine production will increase, whereas the pro-inflammatory cytokine production will decrease. As exposure to *S.aureus* components increases, macrophages will exhibit an elongated phenotype over time. Lastly, I predict that cytotoxicity will not increase and cell viability will not decrease as *S.aureus* components lack a toxin and are not known to cause cell death.

III. LITERATURE BACKGROUND

Gram Positive Bacteria

A Gram positive bacterium, like *S.aureus*, stains a bright purple color as the crystal violet stain is held in by the thick peptidoglycan layer of the cell wall (Brown et al., 2015). As reviewed by Brown et al., 2015, the cell wall of *S.aureus* is fairly simple. Essentially, the cell wall of *S.aureus* consists of the gram positive thick layer of peptidoglycan with teichoic acid, and lipoteichoic acids attached to the cell membrane via a diacylglycerol linkage (Brown et al., 2015) as shown in figure 1. During infection, the cell wall of *S.aureus* will be recognized by the immune system and allows it to be taken up by macrophages.

Course of Infection

In the event of infection, the immune response is composed of two parts: the innate and adaptive response. The first twenty-four hours are in part the most important in clearing a pathogen from the host. Within the first few hours of infection, *S.aureus* are phagocytized by phagocytic cells such as macrophages which are circulating in the bloodstream (Wardenburg et al., 2006). Once the bacteria are phagocytized, macrophages secrete inflammatory cytokines to recruit neutrophils and other phagocytic cells to the area to help limit the spread of infection (Wardenburg et al., 2006). These signals are induced by the binding of pathogen-associated molecule patterns (PAMPs) to receptors such as Toll-like receptors (TLRs) or nucleotide-binding oligomerization domain-like receptors

(NOD) receptors which will then begin transcription of inflammatory cytokines and chemokines to attract more cells to the area (Wardenburg et al., 2006). Unfortunately, the inflammation caused by these cytokines may cause tissue damage. As a balance to the inflammation, an anti-inflammatory response occurs throughout an infection to help reduce excessive inflammation and reduce the production of inflammatory cytokines (Frodermann et al., 2011).

Peptidoglycan

Peptidoglycan is the primary component of a gram positive bacterium cell wall. The peptidoglycan layer of the cell wall defines *S.aureus* as a gram positive bacterium, as it is very thick (Girardin et al., 2003). The main difference in gram positive peptidoglycan and that of gram negative bacteria is in the amino acid makeup of the peptides: gram positive bacteria have a lysine at the third position, whereas gram negative bacteria have a diaminopimelic acid (Girardin et al., 2003). *S.aureus* peptidoglycan consists mostly of N-acetylglucosamine and N-acetylmuramic acid that are linked together to form a thick, rigid layer that protects the cell (Girardin et al., 2003).Throughout the life cycle of the bacteria, the peptidoglycan wall is constantly degraded and synthesized as the cell divides and persists throughout infection (Girardin et al., 2003).

It was previously believed that peptidoglycan activated the immune response via TLR-2 (Dziarski and Gupta, 2005). Recently, it was discovered that peptidoglycan activates a

macrophage via intracellular NOD receptors such as NOD1 and NOD2 (Dziarski and Gupta, 2005) (Figure 3). Specifically, NOD2 receptors recognize muramyl dipeptide (MP), whereas NOD1 receptors recognize meso-diaminopimelic acid- containing peptides- each are peptides present in both gram positive and gram negative bacteria peptidoglycan (Girardin et al., 2002). In order for a NOD receptor to recognize the peptidoglycan of *S.aureus*, the peptidoglycan needs to be inside the cytosol as NOD receptors are cytosolic (Ratner et al., 2007). As a macrophage degrades *S.aureus*, the degraded peptidoglycan from the cell will be recognized by the cytosolic NOD receptor and this will trigger a signaling cascade to begin transcription of cytokines to initiate an immune response.

Lipoteichoic Acid

Teichoic acids are a class of gram positive cell wall components, lipoteichoic acid are common throughout the cell wall of *S.aureus* (Morath et al., 2002). LTA is an amphiphilic molecule that is linked to to the cell membrane of *S.aureus*, commonly expressed during cell growth, especially during infection and causes a large immune response in its pure form (Schroder et al., 2003). Generally, gram positive lipoteichoic acids are composed of diacylgelyerol glycolipids that are covalently coupled to a polymeric backbone (Schroder et al., 2003). The structure among gram positive LTA differs slightly amoung species, *S.aureus* LTA is composed of repeating units of D-

alanine and α-D-N-Acetyl glucosamine that are linked to a linear 1-3-polyglycerophophstae chain (Schroder et al., 2003).

Recently, the immunostimulatory effects of *S.aureus* LTA have been questioned (Morath et al., 2002). Most studies were done using heat-killed LTA, and it has been shown to induce TLR-2 response which activates the transcription factor nuclear factor- κB (NF-κB) to begin transcription of cytokines and chemokines (Schroder et al., 2003) (Figure 4). Unfortunately, it is very difficult to purify LTA from *S.aureus* without contamination by an endotoxin (Morath et al., 2002). However, when done successfully, purified LTA has been shown to induce production of both inflammatory and anti-inflammatory cytokines such as TNF-α, IL-1β, IL-6, and IL-10 in whole blood models (Morath et al., 2002). LTA exerts a very low immunostimulatory effect when compared to PGN and LPS (Morath et al., 2002).

Cytokines

Tumor Necrosis Factor α

Once an antigen such as LTA or PGN binds to its receptor and the signaling cascade for cytokine production occurs, inflammatory cytokines are typically produced first. Inflammatory cytokines play an important role in the immune response as the cytokines attract more cells to the area in order to combat infection (Sullivan et al., 2007). The main inflammatory cytokine produced is tumor necrosis factor α (TNF-α); TNF-α plays a

crucial role in the acute response to infection by a pathogen as it is produced rapidly (Sullivan et al., 2007). Macrophages, cluster of differentiation (CD)-4 T-helper-1, and CD8 cells cells are the primary producers of TNF-α, which stimulate other cells throughout an infection (Sullivan et al., 2007). TNF-α production is primarily studied using LPS treatment as LPS is known to produce a strong inflammatory response (Sullivan et al., 2007). The production of TNF-α is dependent on transcription and specific splicing of regulatory elements such as the TNF-α-converting enzyme which helps control the overexpression of the inflammatory cytokine (Sullivan et al., 2007). Although the TNF-α-converting helps to regulate the expression of TNF-α, the mechanism by which it does so is not very well understood (Sullivan et al., 2007). Other factors that regulate the production of TNF-α include other cytokines such as the inflammatory cytokine IL-10 (Pengal et al., 2006).

Interleukin 10

In order to balance the immune response, anti-inflammatory cytokines such as Interleukin 10 (IL-10) are produced to protect the host from tissue damage that may be caused by excess inflammation (Frodermann et al., 2011). IL-10 is primarily produced by innate immune cells such as macrophages and natural killer cells. However as infection persists, it may be produced by T-cells and B-cells (Verma et al., 2016). IL-10 is important during infection as it can regulate other cytokines. For example, it may inhibit the production of inflammatory cytokines (Hasko et al., 1996).

IL-10 functions in an autocrine manner, regulating its own production. In macrophages, IL-10 is recognized by the IL-10 receptor which then begins a signaling cascade for the amplification of IL-10 production (Shinohara et al., 2014). The amplification of IL-10 involves transforming growth factor-β-activated kinase-1 (TAK1), inhibitor of nuclear factor kappa-B subunit β (IKKB) and caspase recruitment domain-containing protein 11 (CARMA1) to act like an "on switch" for NF-KB signaling (Shinohara et al., 2014). One molecule of IL-10 amplifies its own production, creating a positive feedback loop (Shinohara et al., 2014). However, once the concentration of IL-10 is great enough, negative feedback occurs. As reviewed by Saraiva and O'Garra, 2010, at a high concentration of IL-10, dual-specificity protein phosphatase 1 (DUSP1) is induced which regulates P38 phosphorylation and will inhibit IL-10 production (Saraiva and O'Garra, 2010) (Figure 2). This is a way for the immune system to regulate itself to prevent future damage and disease.

Cytokine Secretion

After transcription of cytokines occurs, the synthesis and excretion of cytokines from the cell is similar to how most cells produce proteins. After synthesis, cytokines are collected in the Golgi complex before movement out of the cell (Murray et al., 2005). Unlike some proteins, cytokines are not synthesized and stored into granules before being released from the cell (Murray et al., 2005). Cytokines are released in a rapid process that is

limited by the expression of soluble N-ethylmaleimide sensitive fusion (NSF) attachment proteins (SNAREs), which are involved in the fusion of vesicles to the macrophage cell wall (Murray et al., 2005). As SNARE expression is increased, the rate of cytokine secretion increases (Murray et al., 2005). Cytokines collect at the Golgi complex before vesicles are formed to transport cytokines from the cell (Murray et al., 2005).

Intracellular Flow Cytometry

Flow cytometry is an efficient way to measure several characteristics of cells during a *S.aureus* infection. In previous studies, intracellular cytokines such as TNF-α and Interleukin-8 were measured after treatment with *S.aureus* LTA (Aulock et al., 2003). Aulock and colleagues focused their study on monocytes isolated from female C57BL/6 mice (Aulock et al., 2003). In this study, flow cytometry was used to measure cytokine levels in arbitrary units followed by quantification by ELISA (Aulock et al., 2003). In initial experiments, Aulock and colleagues exposed monocytes to *S.aureus* LTA for a time period of 30 minutes and 4 hours at a concentration of 10 μg/mL before examination by flow cytometry (Aulock et al., 2003). 10 μg/mL of LPS and LTA induced similar levels of TNF-α and IL-8 after five hours (Aulock et al., 2003). Using ELISA, TNF-α, IL-8 and IFN-γ secretion was measured over 24 hours after exposure to various concentrations of *S.aureus* bacteria, *S.aureus* LTA, *E.coli* bacteria, and *E.coli* LPS (Aulock et al., 2003). The findings of this study suggests that *S.aureus* LTA has very different qualities than *E.coli* LPS. Unlike suggestions of earlier studies, LTA may

induce large quantities of chemoattractants, but does not strongly activate neutrophils and other innate immune cells (Aulock et al., 2003). Aulock and colleagues concluded that *S.aureus* LTA plays an important role in recruitment of innate immune cells to the area of infection, and it causes macrophages to secrete cytokines (Aulock et al., 2003).

In several previous studies, flow cytometry has been used to study phagocytosis of *S.aureus* by macrophages (Deshmukh et al., 2008). Deshmukh and colleagues labeled *S.aureus* with Alexa 344 before exposing them to bone-marrow macrophages for thirty minutes (Deshmukh et al., 2008). Throughout infection, macrophages engulf bacteria, such as *S.aureus*, before degrading the pathogens initiating a response via NOD signaling inside the cell (Deshmukh et al., 2008). This study used wild-type and NOD knock out mice to observe the role that NOD signaling plays in phagocytosis and cytokine production (Deshmukh et al., 2008). Intracellular flow cytometry was used to measure fluorescence intensity which corresponded to the amount of *S.aureus* that had been phagocytized by each cell (Deshmukh et al., 2008). The phagocytosis assay showed that NOD knockout mice had a significant decrease in *S.aureus* phagocytosis in both bone-marrow derived neutrophils and macrophages (Deshmukh et al., 2008). Unfortunately, Deshmukh and colleagues did not use flow cytometry to determine cytokine production. An enzyme-linked immunosorbent assay (ELISA) was used to observe cytokine production. The levels of TNF-α in NOD knockout mice were slightly increased, levels of IL-10 did not differ from control mice (Deshmukh et al., 2008).

Cytoskeleton

The cytoskeleton of a macrophage plays a large role in cell mobility and function. When macrophages are activated into either the M1 or M2, they express different degrees of elongation (McWhorter et al, 2013). While both phenotypes are elongated, M2 macrophages were shown to have an increased elongation when compared to M1 (McWhorter at el., 2013). Macrophage microtubules are composed of alternating units of α- and β-tubulin (Robinson and Vandre, 1995). Macrophage microtubules rapidly depolymerize as most microtubules have a half life ranging from five to fifteen minutes (Robinson and Vandre, 1995). Additionally, microtubules are regulated by extracellular signals, such as inflammatory or anti-inflammatory cytokines which allow the microtubules to respond by changing the cell morphology (Robinson and Vandre, 1995). Microtubules are typically more stable once acetylated (Binker et al.,2007). When macrophages are polarized to the M1 phenotype, more acetylated α-tubulin has been observed (Binker et al., 2007). Increased acetylated tubules indicates that the macrophage microtubules are more stable (Binker et al., 2007).

Another primary cytoskeletal component important in macrophages during infection is actin. Actin is a primary component in many eukaryotic cells, including murine macrophages (Dominguez and Holmes, 2011). As reviewed by Jiang and colleagues, the structure of F-actin was shown to be two tightly twisted strands of pre-polarized F-actin forming a helical polar filament (Jiang et al., 2016). In macrophages, actin plays a

primary role in phagocytosis, phagosome formation, as well as fusion events (McWhorter et al., 2013).

When actin polymerization is inhibited by drugs, phagocytic function is also inhibited (McWhorter et al., 2013). Actin plays a primary role in distinguishing M1 and M2 macrophages (McWhorter et al., 2013). In M1, inflammatory macrophages, F-actin has been shown to cluster around the nucleus; whereas in M2, anti-inflammatory macrophages, F-actin has been shown to be primarily located around the outer edge of the cell (Vereyken et al., 2011). Additionally, M2 macrophages have been shown to have more F-actin present than M1 macrophages, suggesting that actin must be important in the elongation and adhesion proccesses of macrophages, properties induced by anti-inflammatory cytokines (McWhorter et al., 2013).

Immunofluorescence

Macrophages are known to have three general phenotypes: M0, M1, and M2 which may be determined by cytokine production as well as morphology (McWhorter et al., 2013). In a previous study, levels of F-actin and α-tubulin were studied in both M1 and M2 macrophages (McWhorter et al., 2013). McWhorter and colleagues found that within 24 hours post stimulation, M1 macrophages exhibited a circular profile, whereas M2 macrophages appeared more elongated (McWhorter et al., 2013). Similar to this study, immunofluorescent staining was done as well as Western blotting to evaluate polarization

(McWhorter et al., 2013). Characteristics such as inducible nitric oxide synthase and arginase-1 were observed via immunofluorescence staining for inflammatory and anti-inflammatory phenotypes, respectively (McWhorter et al., 2013). The cells which showed elongation via immunofluorescent staining also exhibited very high inflammatory cytokines, therefore the authors concluded that anti-inflammatory M2 macrophages exhibit an elongated phenotype (McWhorter et al, 2013). When macrophages were transformed into M1 and M2 macrophages, a western blot showed that M1 macrophages exhibited more α-tubulin than M2 macrophages, whereas M2 macrophages exhibited more polymerized F-actin (McWhorter et al., 2013). The study done by McWhorter and colleagues concluded the change in phenotype by macrophages correlates to inflammatory and anti-inflammatory states when stimulated by cytokines.

Cytotoxicity

S.aureus is known for several virulence factors, such as antibiotic resistance and toxin production, which allows it to sustain an infection in a host. Several strains of *S.aureus* are known to produce toxins which are toxic to host cells, especially *S.aureus* α-toxin which is known to kill host immune cells (Valeva et al., 1997). α-toxin is known to form spontaneous pores in a target cell's membrane (Valeva et al., 1997). In human and rabbit lymphocytes, a transmembrane β-barrel was formed after exposure to α-toxin (Valeva et al., 1997). However, human granulocytes are resistant to the pore-forming abilities of the α-toxin (Valeva et al., 1997). Additionally, *S.aureus* secrete membrane vesicles (MVs)

containing a variety of proteins including Protein A to host cells (Jeon et al., 2016). In a previous study, Jeon and colleagues had concluded that MVs are responsible for cell cytotoxicity after treating a HeLA cell line with *S.aureus* membrane vesicles (Jeon et al., 2016). As the concentration of MVs increased, the number of living cells decreased (Jeon et al., 2016). Previous studies have shown that MVs exhibit varying levels of cytotoxicity in different cell types (Jeon et al., 2016). The differing cytotoxicity levels may be due to the variety of proteins present in MVs, some host cells may have a resistance to proteins found in MVs (Jeon et al., 2016; Valeva et al., 1997).

IV. MATERIALS AND METHODS

Cell Culture

RAW264.7 murine macrophage cells (ATCC, Manassas, VA) were originally obtained from Abelson murine leukemia virus-induced tumors in adult male BALB/c mice were used in this study. The RAW264.7 cell growth pattern is adherent; in order to passage cells, a small cell scraper (Fisher Scientific, Pittsburgh, PA) was used to remove cells from the interior of a vented BioLite flask (Fisher Scientific, Pittsburgh, PA). Cells were passaged three to four times weekly in a medium containing Dulbecco's Modified Eagle's Medium (DMEM), 10% Fetal Bovine Serum (FBS), and 10mM Hepes buffer before incubation at 5% Carbon dioxide and 37°C with 100% humidity until 60% confluency is reached. Confluency is estimated via visual observation of the cells growth on the flask. Macrophage cell type was confirmed by staining for CD11b macrophage marker, observed by immunofluorescence microscopy (Figure 5).

Cell Viability

Cells were grown to approximately 60% confluency prior to treatment time period. After each treatment period, cells were removed from the flask. Cells were then resuspended in 10% FBS in DMEM before 10 μL of cell suspension was added to 20uL of trypan blue (Fisher Scientific, Pittsburgh, PA). To count cells, 10uL were placed onto a hemacytometer and observed under a microscope at 10x magnification. Cells which are dead are stained by trypan blue, whereas cells which are alive do not take up the dye. The

number of live cells versus dead cells are used to determine the cell viability. All experiments used cell populations with 60% viability.

$$\left(\frac{Number\ of\ cells\ in\ five\ squares}{5}\right) * 25 * 2 * 10{,}000 = Total\ Viable\ Cell\ Concentration$$

Equation 1: Equation used to determine the concentration of viable cells within a culture

Cell Treatments

Staphylococcus aureus cell wall components lipoteichoic acid and peptidoglycan were purchased from Invivogen (San Diego, CA). Each cell wall component used in a treatment of 5 μg/mL. Interleukin-10 (IL-10) and Escherichia coli Lipopolysaccharide (LPS) were used as positive controls for anti-inflammatory and inflammatory treatments, respectively. For positive controls, 100 ng of IL-10 was used to transform macrophages into the M2 anti-inflammatory phenotype; 100 ng of LPS was used to transform macrophages into the M1 inflammatory phenotype. Experiments were performed using *S.aureus* components over the course of 24 hours, with cells removed at six hour intervals. Experimental treatments are shown in Table1.

Treatment	Concentration
Negative	No Treatment

Interleukin-10 (Positive Control)	100 ng/mL
E.coli Lipopolysaccharide (Positive Control)	100 ng/mL
S.aureus Lipoteichoic Acid	5 µg/mL
S.aureus Peptidoglycan	5 µg/mL
S.aureus Lipoteichoic Acid & Peptidoglycan	5 µg/mL

Table 1: Table showing the treatments for each experimental group

Flow Cytometry

Cells were grown to approximately 60% confluency before treatment *S.aureus* experimental groups and controls. Due to the negative feedback loop in the production of IL-10, RAW264.7 macrophages were treated with 100 ng of IL-10 approximately thirty minutes prior to running flow cytometry for the positive control treatment. In preliminary experiments, cells treated with IL-10 for 6 hours or more did not have any intracellular IL-10 present. Experimental groups had incubation times ranging from six to twenty-four hours, the appropriate incubation period depended on the total time for the trial. In the last four hours of incubation, Brefeldin A (BFA) (BioLegend,San Diego, CA) solution was added to the cells at a concentration of 5 µg/mL. BFA solution inhibits cytokine secretion out of the cell. After the appropriate treatment period, cells were harvested and counted via a hemocytometer.

Approximately two million cells were placed in microcentrifuge tubes and pelleted via centrifugation. Cells were fixed with Fixation Buffer (BioLegend,San Diego, CA) for twenty minutes at room temperature. Following fixation, all samples were washed with 1X Permeabilization Wash Buffer (BioLegend,San Diego, CA) three times at room temperature. Next, cells were stained with anti-IL-10, anti-TNF-α , or appropriate isotype controls (Fisher Scientific, Pittsburgh, PA) (Table 2) for twenty minutes at room temperature. Following staining, samples were washed before resuspension in Cell Staining Buffer (BioLegend,San Diego, CA) and run on an Accuri C6 Flow Cytometer at medium speed with a flow rate of 35 μL per minute, and a core size of 16 μm for 50,000 events.

Antibody	**Concentration/Dilution**	**Company**
FITC Anti-IL-10	0.25 μg/mL	Thermo Scientific, Pittsburgh, PA
Rat/ IgG2bκ (IL-10 Isotype)	0.25 μg/mL	Thermo Scientific, Pittsburgh, PA
FITC Anti- TNF-α	0.06 μg/mL	Thermo Scientific, Pittsburgh, PA
Rat/ IgG1κ (TNF-α Isotype)	0.06 μg/mL	Thermo Scientific, Pittsburgh, PA
α - β –Tubulin #2148 (Primary Tubulin Antibody)	1:50	Cell Signaling Technology, Danvers, MA
Anti-Rabbit IgG (H+L), $F(ab')_2$ Fragment (Alexa Fluor 488 conjugate) (Secondary Tubulin antibody)	1:250	Cell Signaling Technology, Danvers, MA
Texas Red-Phalloidin (F-actin tag)	1:300	Cell Signaling Technology, Danvers, MA

Anti- CD11B [M1/70] (Primary Antibody for Macrophage Marker)	5 μg/mL	Abcam, San Francisco, CA
Goat Anti-Rat IgG H&L (Alexa Fluor 488) (Secondary Antibody for Macrophage Marker)	2 μg/mL	Abcam, San Francisco, CA

Table 2: Table showing the concentration of antibodies used for flow cytometry and immunofluorescence staining

Histogram Analysis

To analyze the histograms created from the Accuri C6 Flow Cytometer, FCS Express 6 Reader was used. Percent differences were calculated by overlaying each treatment histogram onto the negative control histogram, using the histogram subtraction tool. This positive percent difference represents the difference between the number of cytokines produced by each treatment group and the negative control.

Immunofluorescence Staining

Cells were grown to 60% confluency before approximately 5,000 cells were transferred to Ibidi 12-well chamber slides (Ibidi USA, Fitchburg, WI) in a final volume of 250 μL of medium. Cells were incubated in the wells overnight at 37°C to allow attachment to the slide. After incubation, the old medium was removed and cells treatment was applied to cells for each experimental time period ranging from six to twenty-four hours (Table

1). After each experimental time period, the treatment solution was aspirated and cells were washed with phosphate buffered saline (PBS) twice before fixation with 4% paraformaldehyde for 15 minutes at room temperature. Cells which were used for cytoskeletal staining underwent permeabilization with 0.2% Triton at room temperature for ten minutes. Following permeabilization, cells were washed with PBS before treatment with blocking buffer for an hour at room temperature.

Following blocking, cells were washed with 1% Bovine Serum Albumin (BSA) before primary αβ-tubulin antibody was added to each well. The primary antibody was incubated at room temperature for one hour. After this incubation, the secondary fluorescent antibodies for αβ-tubulin was added and was incubated for one hour at room temperature. After incubation, the cells were washed with 1% BSA. Next, the Texas-Red phalloidin label for F-actin was added and incubated for one hour. After incubation, the antibody solution was removed and cells were washed three times with 1% BSA. In preparation for viewing, the cells were allowed to dry before the silicone well chambers were removed. Once dry, the cells were imaged on the Olympus Epi Fluorescence Spot microscope at 465 nm for αβ-tubulin and 565 nm for Phalloidin labeled F-actin at 40x magnification.

Additionally, macrophage classification was determined using immunofluorescence staining for CD11b (Figure 5), a known macrophage surface marker using the same method to confirm cell type (Lumeng et al., 2007).

Image Analysis

Image analysis was done using ImageJ software. Raw black and white images were uploaded into ImageJ. The background fluorescence was subtracted from the image which allows for the overall mean intensity of the image to be calculated. This mean fluorescence intensity was then divided by the number of cells in each image to determine the mean fluorescence intensity per cell.

Cytotoxicity

Cells were grown to 60% confluency before approximately 200,000 cells were treated for the appropriate experimental group and time point. After each experimental time period, supernatants were collected from each group and then frozen at -80°C until plated. For control groups, approximately 200,000 cells were transferred into a 96 well plate (Corning Incorporated, Corning, NY) containing 200 μL of medium and incubated overnight for cells to adhere. The maximum release group was treated with 20uL of 10% Triton X-100 (Cayman Chemical, Ann Arbor, MI), LDH positive controls contained no cells and only 20uL of LDH, and the spontaneous release group only contained cells with no additional treatment. In a new 96 well plate, 100 μL of each treatment group was

added to each well followed by 100 µL of reaction solution (Cayman Chemical, Ann Arbor, MI). Wells were incubated at 37°C for twenty minutes before being read on the Softmax-Pro Plate Reader at 490 nm to determine the optical density of each group. Percent cytotoxicity was determined using Equation 2.

$$\frac{(Experimental\ OD) - (Spontaneous\ OD)}{(Maximum\ Relsease\ OD\ ) - (Sponetaneous\ OD)} * 100 = \%Cytotoxicity$$

Equation 2: Equation used to convert raw optical density to percent cytotoxicity

Statistical Analysis

Statistical significance was calculated using a One-Way ANOVA (Sigmaplot13.0); all experiments were done at least three times. Error bars were calculated using standard error of the mean.

V. RESULTS

Polarized Macrophages Exhibited Morphological Differences and Higher Cytokine Production When Compared to Control Macrophages

As inflammatory positive controls, RAW264.7 macrophages treated with LPS exhibited high TNF-α production over each time period as exhibited as percent difference from the negative control cells (Figure 6). TNF-α production was highest at six hours while decreasing at each six-hour point over the twenty-four-hour period (Figure 6). The anti-inflammatory positive control for cytokine production required treatment at a short time period. RAW264.7 macrophages treated with IL-10 exhibited high IL-10 production after treatment for thirty minutes (Appendix Figure 3).

When RAW264.7 macrophages were treated with LPS as an inflammatory positive control, cells exhibited the M1 phenotype with more circular profile with few elongated cells over 24 hours at 6 hour intervals (Figures 7, 8, 9, 10). When cells were treated with IL-10 as an anti-inflammatory positive control, cells appeared more elongated as the treatment time periods progressed (Figures 7, 8, 9, 10). M1 and M2 macrophages both displayed visible vacuoles and F-actin accumulating around the outside of the cells (Figures 7, 8, 9, 10).

Inflammatory Cytokine Production over 24 Hours

Production of the inflammatory cytokine, TNF-α, was measured by percent differences from the negative control via flow cytometry. TNF-α production was highest at six hours before decreasing over six hour intervals until the lowest production at twenty-four hours (Figure 6). Macrophages treated with LTA produced less TNF-α production, cells treated with a combination of LTA and PGN produced higher levels of TNF-α production when compared to treatments with individual *S.aureus* cell wall components (Figure 6).

Anti-Inflammatory Cytokine Production over 24 Hours

Anti-inflammatory cytokine IL-10 production was measured by percent differences from the negative control via flow cytometry. IL-10 production was lowest at six hours of exposure to *S.aureus* components and increased overtime (Figure 11). Macrophages treated with LTA produced less IL-10 compared to cells treated with a combination of LTA and PGN (Figure 11). The highest production of IL-10 was observed between 12 and 18 hours (Figure 11).

Cytotoxicity and Viability of Macrophages After Exposure to *S.aureus* Components

RAW264.7 macrophages exhibited no significant difference in cytotoxicity over twenty-four hours of exposure to *S.aureus* cell wall components when measured by an LDH Cytotoxicity assay (Figure 12). Cells treated with LPS exhibited higher cytotoxicity but the percentage was not significant when compared to other treatment groups (Figure 12).

When cell viability was measured via trypan-blue staining, LPS positive controls exhibited a lower percent of viable cells when compared to other groups at each time period over twenty-four hours (Figure 12). Macrophages when treated with *S.aureus* cell wall components exhibited lower percentages of viable cells, however not at a significant level when compared to negative controls (Figure 12).

Morphological Changes Due to Exposure to *S.aureus* Components over 24 Hours

At six hours of exposure, macrophages appeared to be more rounded after treatment with *S.aureus* components, exhibiting an M1 phenotype (Figure 7). As exposure time progressed, cells appeared more elongated like the M2 phenotype at twenty-four hours (Figures 7, 8, 9, 10).

Fluorescence intensity of α-β tubulin showed no significant increase or decrease over twenty-four hours (Figure 13). However, cells treated with PGN only appeared in value to have higher intensity of bound α-β tubulin antibody (Figure 13). Fluorescence intensity of F-actin showed a significant increase of F-actin intensity. Similar to α-β tubulin, PGN showed the highest amount of F-actin intensity (Figure 14). Cells treated with PGN showed a significant increase in F-actin when intensity was compared between six and twenty-four hours (Figure 14). At twenty-four hours, the mean fluorescence intensity of F-actin was the greatest (Figure 14).

VI. DISCUSSION

In this study, RAW264.7 murine macrophages were exposed to *S.aureus* cell wall components for exposure times ranging from six to twenty-four hours. When exposed with *S.aureus* components, macrophages did not exhibit a significant decrease in cell viability when compared to negative controls (Figure 12), nor a significant increase in cytotoxicity (Figure 12). Consequently, any changes observed in macrophage cytokine production or microfilament rearrangement were found in cells with greater than 60% viability.

Inflammatory cytokine production was analyzed by the levels of intracellular TNF-α in macrophages by flow cytometry. TNF-α production peaked at six hours before a large decline at twelve hours, macrophage production of TNF-α then increased again at eighteen hours before another decline at twenty-four (Figure 6). This pattern may be due to the cells ability to phenotype-switch to produce IL-10 in order to balance the inflammatory and anti-inflammatory response to prevent tissue damage (Frodermann et al., 2011). When treated with *S.aureus* components, intracellular TNF-α production appeared to be highest after treatment with PGN and a combination of both LTA and PGN (Figure 6). Over each time period, macrophages treated with LTA exhibited lower TNF-α production. If this experiment were to be done in a mouse model, the immune cells would follow a similar pattern with a decrease in inflammatory cytokines after six hours to prevent tissue damage from occurring (Frodermann et al., 2011). As the

cytotoxicity does not significantly increase, the decline in cytokines at twenty-four hours is not due to cell death (Figure 6).

The anti-inflammatory positive control required analysis at thirty minutes after treatment. In preliminary experiments, when cells were analyzed by flow cytometry after each experimental time period, there was no difference between the treated and untreated cells in cytokine production. While IL-10 does have a positive feedback loop where IL-10 induces the production of more IL-10, a negative feedback loop also exists (Saravia and O'Garra, 2010) (Figure 2). As each flow cytometry experiment was run using approximately two-million cells, the negative feedback loop was induced due to the number of cells producing an exponential amount of IL-10 (Saravia and O'Garra, 2010). As IL-10 is regulated in an autocrine manner, IL-10 produced by macrophages induced more production resulting in an exponential amount of IL-10 present in the medium. The large number of cells producing IL-10 induced the negative feedback loop, therefore the positive control needed to be tested at a shorter time period. As the Positive control (Appendix Figure 3) in this experiment was used to determine the specificity of the antibody binding to IL-10, the shortened positive control time period was acceptable.

At six hours, the intracellular IL-10 production was the lowest when compared to all time periods when TNF-α peaked. Intracellular IL-10 production peaked between at 12 and 18 hours before declining at 24 hours (Figure 11). *S.aureus* LTA induced the highest IL-

10 production at eighteen hours, whereas PGN induced the highest production at 12 hours (Figure 11). Interestingly, the combination of LTA and PGN maintained similar levels at both 12 and 18 hours before decreasing at twenty-four hours (Figure 11). Across all time points, LTA induced the lowest IL-10 response (Figure 11). In previous studies, it was found that *S.aureus* LTA did not have a strong immunostimulatory effect (Morath et al., 2002). The findings of Morath and colleagues are consistent with the findings in this study as LTA induced lower IL-10 production across each experimental time points.

Cell morphology was analyzed via immunofluorescence after staining for α-β tubulin or phallodin detection of F-actin. There was no significant increase or decrease in the intensity of α-β tubulin between cells treated with *S.aureus* components as determined by an one-way ANOVA. At six hours, experimental cells displayed the M1 phenotype with the majority of cells had a circular profile (Figure 77) As treatment time increased, each experimental time group displayed M1 cell morphology however M2 morphology increased over time (Figures 7, 8, 9, 10)

Macrophages imaged for Phalloidin detection of F-actin showed significance increases in F-actin intensity with *S.aureus* PGN over time. The intensity in the phalloidin detection of F-actin increased between 6 hours and 24 hours of exposure (Figure 14). McWhorter and colleagues stated that M2 macrophages display more F-actin, and F-actin aggregates towards the outside of the cell (McWhorter et al., 2013). When cells were stained for F-

actin, cells appeared “fuzzy” as the active actin was elongated around the outside of the cell. Individual cells appeared difficult to decipher as the actin was expanded around the outside of the cell, however individual cells were able to be seen when the same cells were viewed for α -β tubulin (Figures 7, 8, 9, 10) This difference in F-actin was only seen in cells treated with PGN, a significant increase did not occur in cells treated with LTA or a combination of LTA and PGN. The data suggests that as macrophages are transformed into the M2 phenotype to produce IL-10, F-actin increases and aggregates towards the outside of the cell.

VII. FUTURE STUDIES

As time progressed in this current study, RAW264.7 macrophages had a higher inflammatory response at 6 hours followed by an anti-inflammatory response at 12 and 8 hours of exposure to *S.aureus* cell wall components. With the current data, it is not possible to determine if cells had undergone a phenotype switch from M1 to M2 macrophages as time progressed, or if a second population of cells were activated at the later time periods. Future studies should include observation and tracking individual macrophages over 24 hours. Under constant observation, individual macrophages should be tracked after treatment with *S.aureus* cell wall components. Cells should be assessed for a circular phenotype or elongation for M1 and M2 phenotype, respectively. A population of approximately 100 cells, tracking individual cells, should be observed for phenotype over 24 hours by real-time microscopy. Results from tracked macrophages should determine if cells were able to convert from an M1 to M2 phenotype or if the increase in anti-inflammatory characteristics was due to two cell populations activating at different time periods.

As the innate immune response to *S.aureus* cell wall components by macrophages was observed in this study, future studies should focus on antigen-presenting cells and antigen presentation to the adaptive immune system. When neutrophils capture *S.aureus* in neutrophil extracellular traps (NETs) the compound 2'deoxyadenosine (dAdo) is toxic to

macrophages (Thammayongsa et al., 2013), causing apoptosis and disruption of the cytoskeleton (Ceruti et al., 2000). Neutrophils are also known to form an aggregate around *S.aureus* during an infection, therefore blocking additional cell migration to the area (Miller and Cho, 2011). Additionally, *S.aureus* has been shown to directly kill dendritic cells as a way to evade immune response (Wu and Wu, 2014). These studies have shown the lack of immune response to *S.aureus* is due, in part, to the inability of the adaptive immune system to be initiated.

Future experimentation to observe the effect of dAdo and inhibitors of dAdo on antigen presenting cells, neutrophils, and dendritic cells is warranted. Macrophages and dendritic cells could be evaluated for antigen-presenting structures such as major histocompatibility complex (MHC) molecules for increases or decreases in expression in vivo (Lin and Peterson, 2010). In vivo experiments involving *S.aureus* infection in mouse skin are useful to evaluating the effect of inhibitors of dAdo as shown by protection from cell death (Thammayongsa et al., 2013). Weekly evaluation, of mice serum and spleen cells would be required for examination of protective adaptive immune responses from *S.aureus* peptidoglycan and lipoteichoic acid. If successful, this may be a treatment for individuals with chronic *S.aureus* infections as a vaccine so that they may develop their own immune responses. A novel treatment using inhibitors of dAdo may be useful as *S.aureus* strains are quickly acquiring resistant

An issue not addressed in the present study is the effect of superantigens produced by toxigenic strains of *S.aureus* on cells. Superantigen removes up to 20% of an individuals T-cell repertoire (Lin and Peterson, 2010). It would be interesting to determine, in future studies, if inhibition of dAdo would provide enough immune protection to inhibit the replication of *S.aureus* to inhibit the secretion of superantigens. As superantigen production occurs approximately 10 to 14 days after infection (Lin and Peterson, 2010), if it were possible to destroy the infection of *S.aureus* via an dAdo inhibitor this may be a novel treatment to prevent superantigen production. Ideally, inhibiting dAdo would allow cells to reach the area of infection without being killed. After approximately 10 to 14 days, *S.aureus* creates a large colony which produces lethal superantigens (Lin and Peterson, 2010). DAdo inhibition would allow the infection to be cleared more quickly by innate immune cells which would normally be destroyed. This treatment may lead to the prevention of many severe infections and deaths of individuals.

VIII. CONCLUSION

The goal of this study was to determine the potential innate immune response by RAW264.7 macrophages to *S.aureus* cell wall components within the first twenty-four hours. The inflammatory response dominated within the first six hours of infection, while the anti-inflammatory response dominated at 12 and 18 hours after exposure to *S.aureus* cell wall components. The pattern of a marked inflammatory response as demonstrated by TNF-α production followed by an anti-inflammatory response of IL-10 production is similar to the in vivo response, as the body would protect itself from excessive inflammation leading to tissue damage. The cells did not have a significant decrease in cell viability measured by tyrpan-blue staining as well as no increase in cytotoxicity measured by LDH secretion. Consequently, cell death was not likely responsible for decreased cytokine production at 24 hours. This may be used as a basis for future studies to determine if the phenotype of the macrophages switches from M1 to M2, as well as the effects of dAdo on cell culture models of macrophage infection by *S.aureus*.

IX. FIGURES

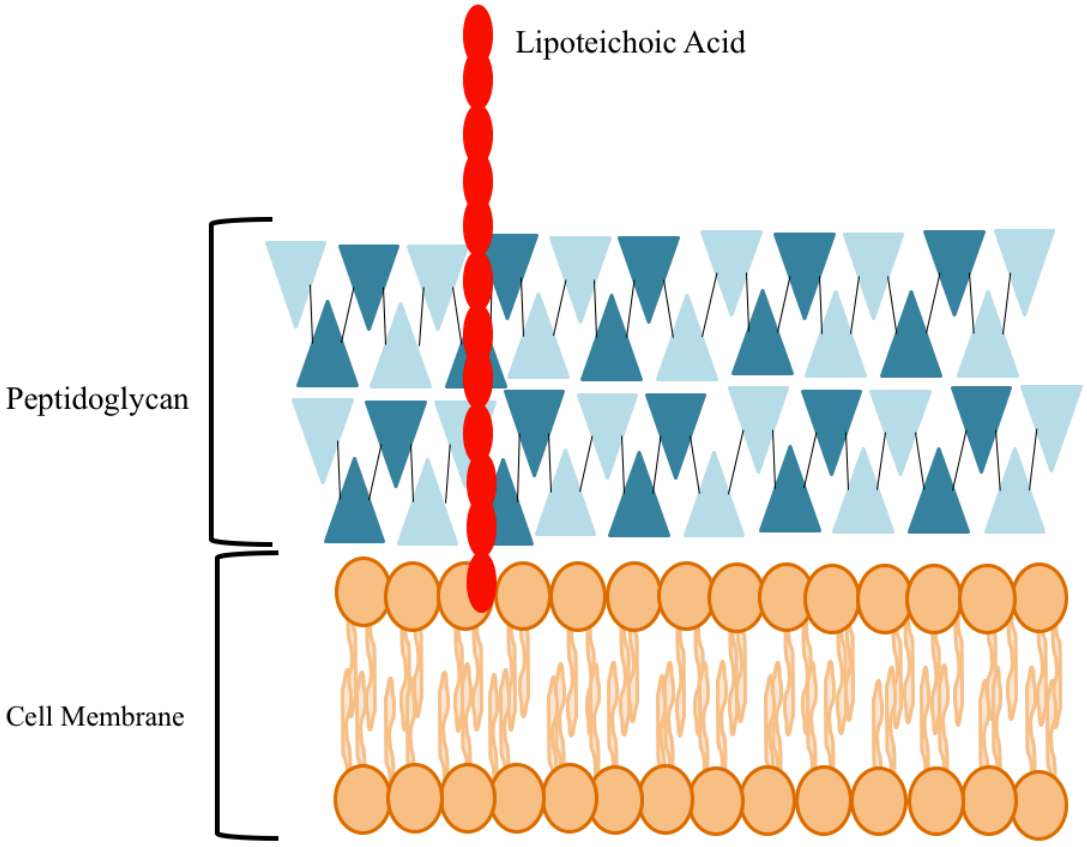

Figure 1: Structure of *S.aureus* peptidoglycan and Lipoteichoic acid. Figure shows the structure of peptidoglycan and lipoteichoic acid, as adapted by Brown and colleagues (Brown et al., 2015). Triangles represent repeating units of N-acetylglucosamine and N-acetyl-acetylmuramic acid (Brown et al., 2015). Red ovals represent lipoteichoic acid (as adapted byBrown et al., 2015).

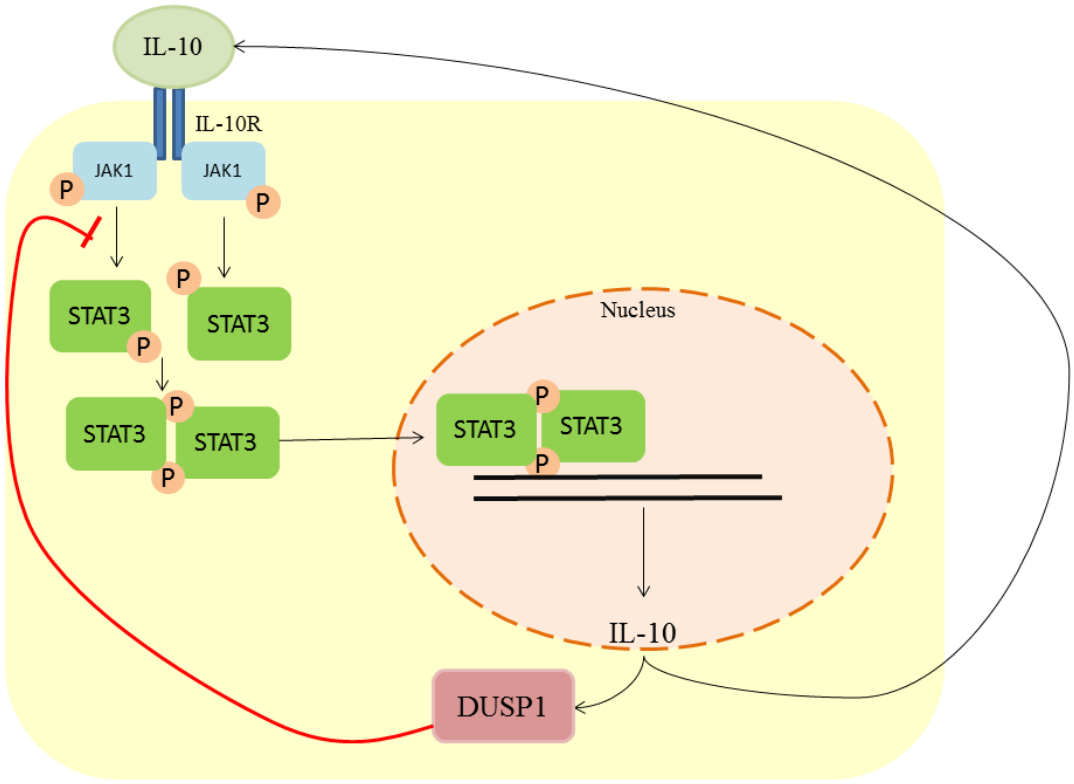

Figure 2: IL-10 Regulation Loop. Figure shows IL-10 positive and negative feedback loop as adapted from Saraiva and O'Garra (Saraiva and O'Garra, 2005). IL-10 positively regulates itself via JAK-STAT signaling, IL-10 is recognized by the IL-10 receptor, when JAK1 becomes phosphorylated, it activates STAT3 via phosphorylation (Saraiva and O'Garra, 2005). When STAT3 is properly phosphorylated, it travels into the nucleus and begins transcription of IL-10 (Saraiva and O'Garra, 2005). However, IL-10 production also activates DUSP-1 which blocks phosphorylation of STAT3 to inhibit IL-10 production (Saraiva and O'Garra, 2005).

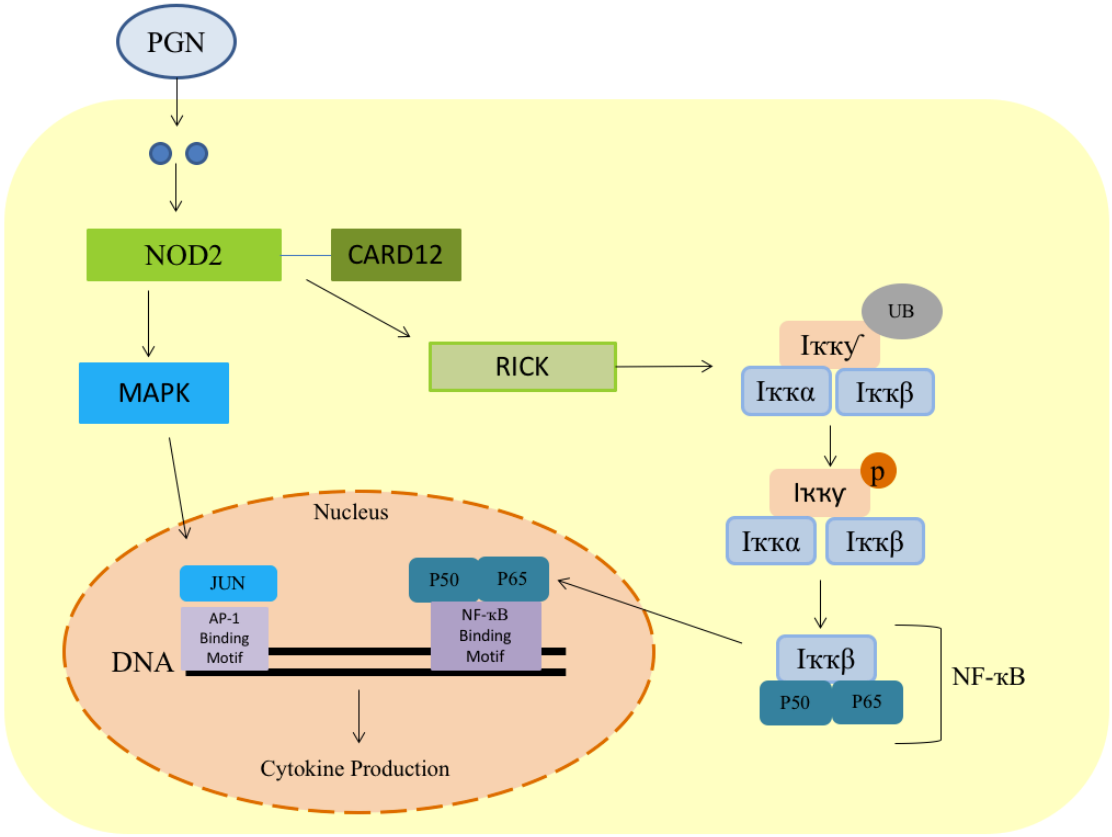

Figure 3: Peptidoglycan macrophage activation via NOD signaling. Figure shows the activation of NOD signaling via *S.aureus* peptidoglycan as adapted by Strober and Colleagues (Strober et al., 2005). Peptidoglycan is brought into the cell, NOD2 recognizes gram-positive peptidoglycan components muramyl dipeptide (Strober et al., 2005). NOD2 recognizes muramyl dipeptide, NOD then recruits CARD12 (Strober et al., 2005). Together, NOD2 and CARD begins a signaling cascade activating RICK, NF- κB and MAPK which will go into the nucleus to begin transcription of cytokines (Strober et al., 2005).

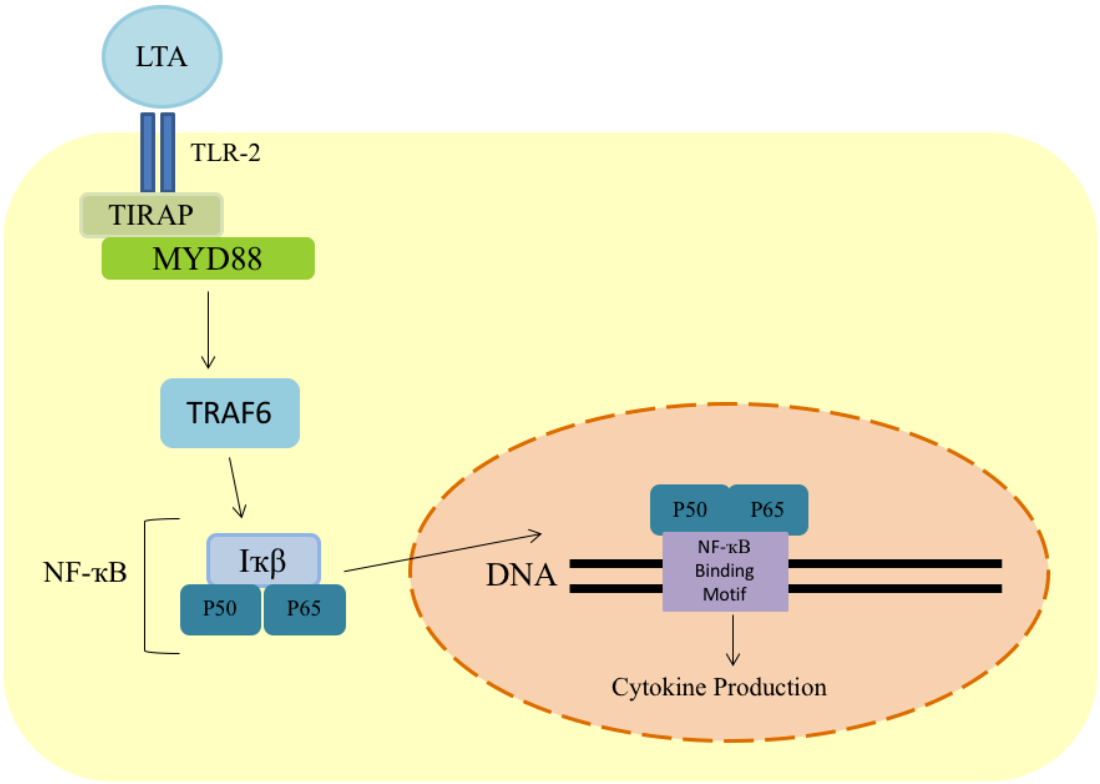

Figure 4: Lipoteichoic acid activates macrophages via TLR-2 signaling. Figure shows the activation of TLR2 signaling via *S.aureus* lipoteichoic acid as adapted by Miller and Cho (Miller and Cho, 2011). Lipoteichoic acid binds to TLR2 which activates TIRAP and MYD88 (Miller and Cho, 2011). TLR2 activation begins a signaling cascade through NF-κB (Miller and Cho, 2011). P50 and P65, NF-KB components, are transported into the nucleus and begin transcription of cytokines (Miller and Cho, 2011).

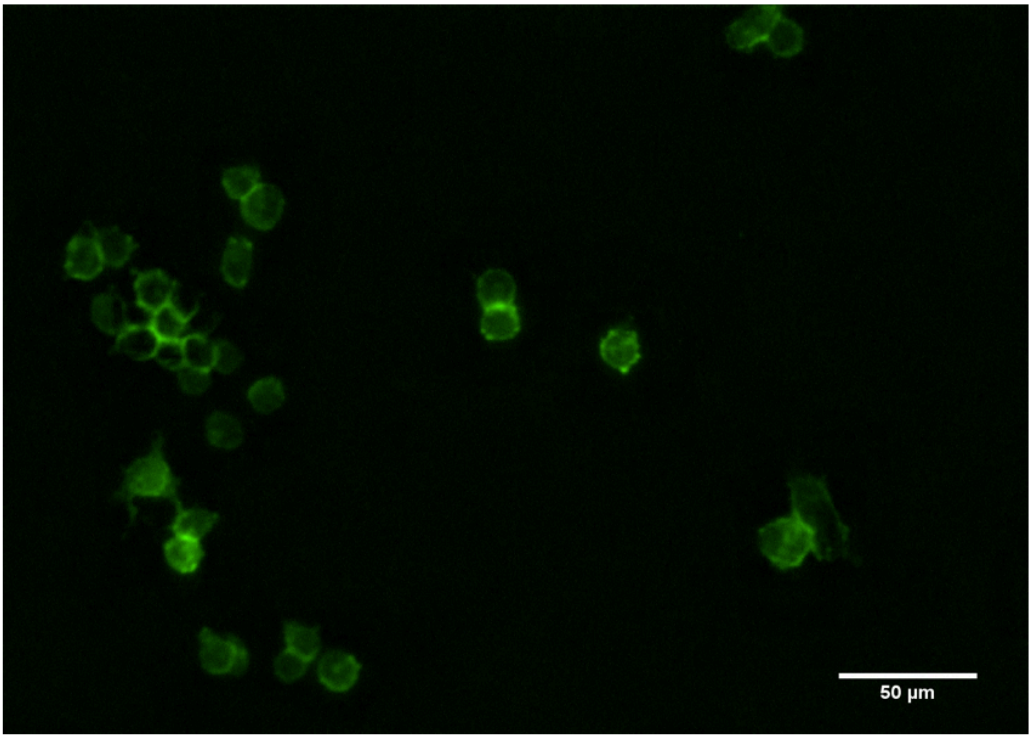

Figure 5: CD11B macrophage marker confirming cell type. Figure shows macrophages as viewed by immunofluorescence microscopy when stained with CD11b (green), a known macrophage marker.

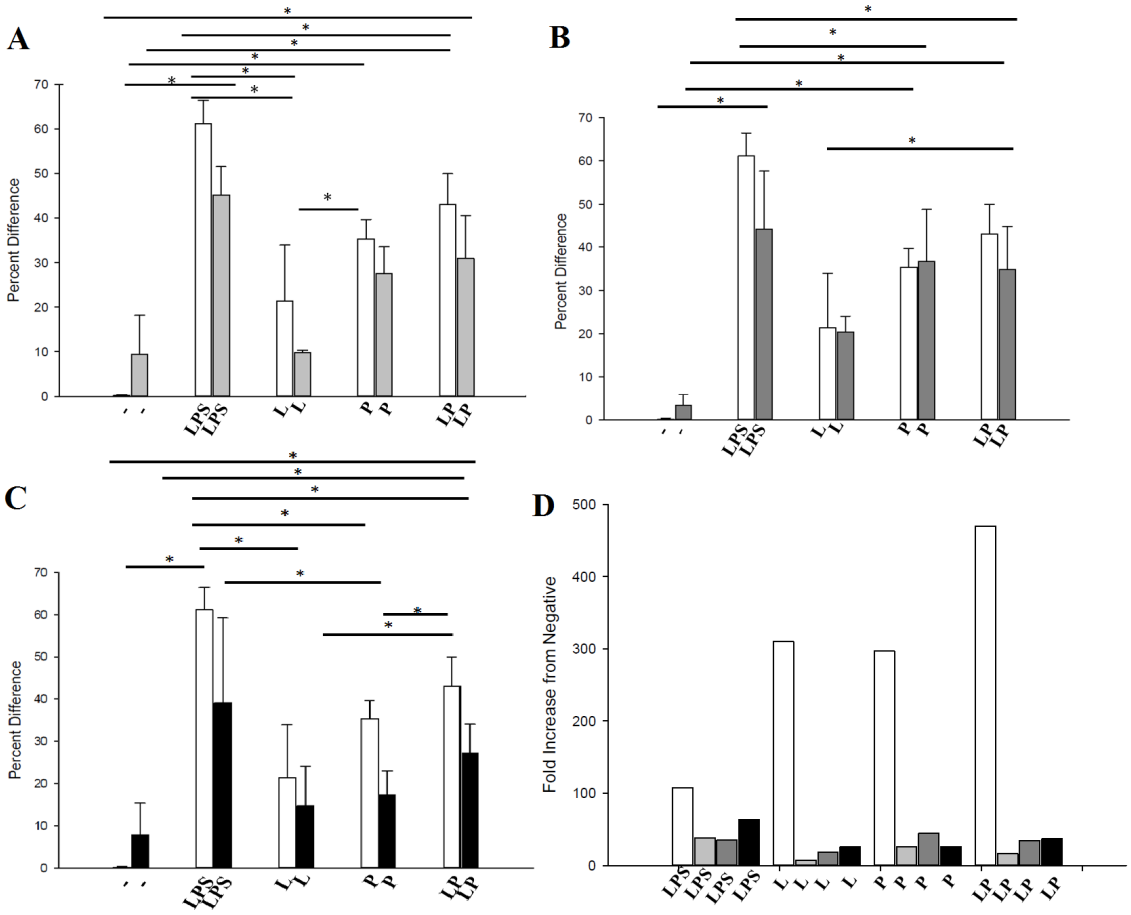

Figure 6: Comparison of intracellular TNF-α production over 24 hours. Figure shows comparison of TNF-α production between (**A**) 6 and 12 hours of treatment, (**B**) 6 and 18 hours of treatment, (**C**) 6 and 24 hours of treatment. Figure **D** shows mean fold increase from negative control cells in intracellular TNF-α production as observed via flow cytometry. Error bars represent standard error of the mean. (* denotes $P<0.05$) (- = Negative control, LPS= Lipopolysaccharide control, L= Lipoteichoic acid, P= Peptidoglycan) (white columns denotes treatment at 6 hours, light grey columns denote treatment at 12 hours, dark grey denotes treatment at 18 hours, and black columns denote treatment at 24 hours)

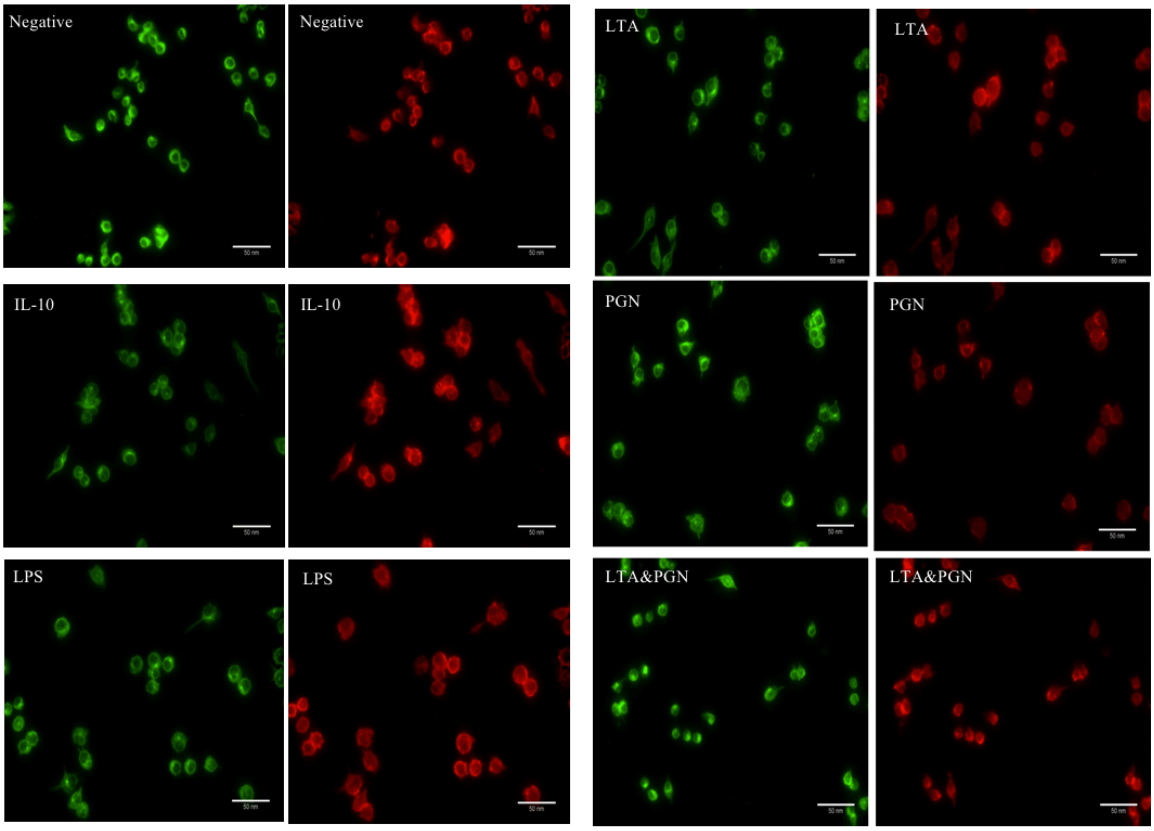

Figure 7: Cell morphology of RAW264.7 macrophages after 6 hours of exposure to *S.aureus* components. Figure shows macrophages at 6 hours of treatment as viewed by immunofluorescence microscopy. Cells were stained for α-β tubulin (green) and F-actin (red). Scale bars represent 50 μm.

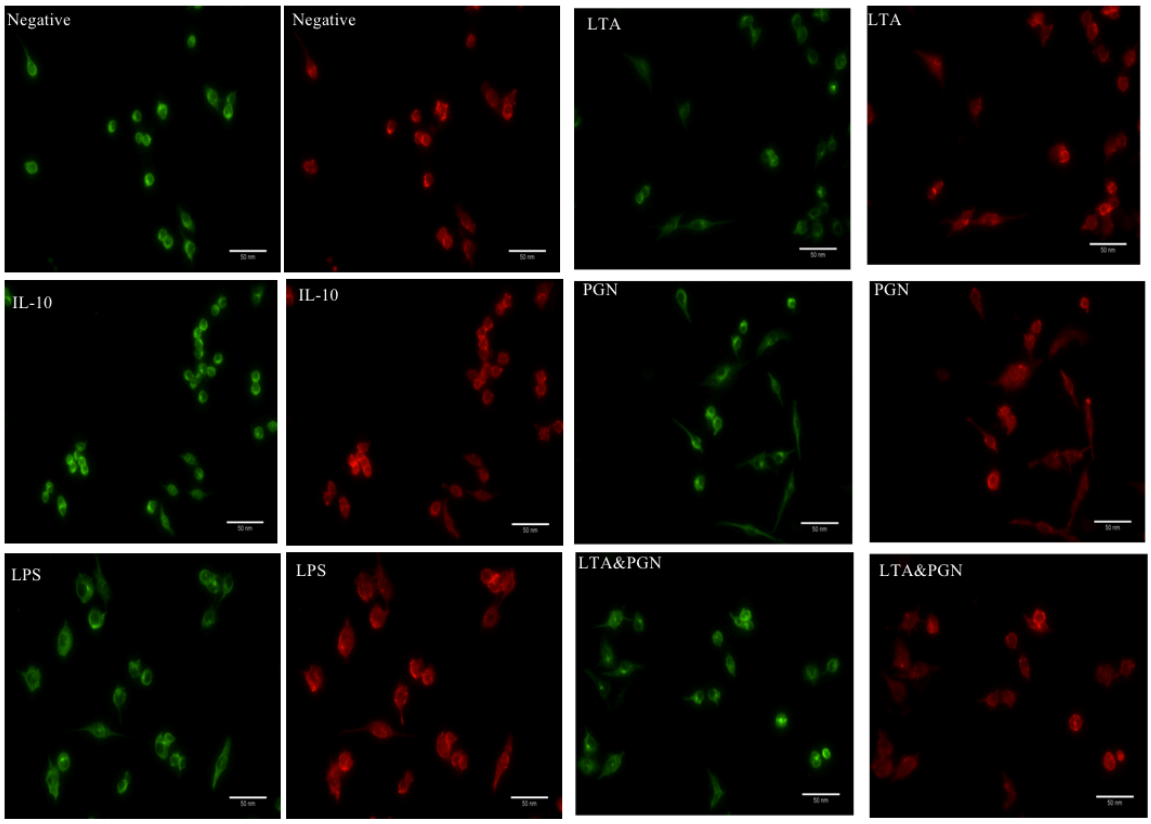

Figure 8: Cell morphology of RAW264.7 macrophages after 12 hours of exposure to *S.aureus* components. Figure shows macrophages at 12 hours of treatment as viewed by immunofluorescence microscopy. Cells were stained for α-β tubulin (green) and F-actin (red). Scale bars represent 50 μm.

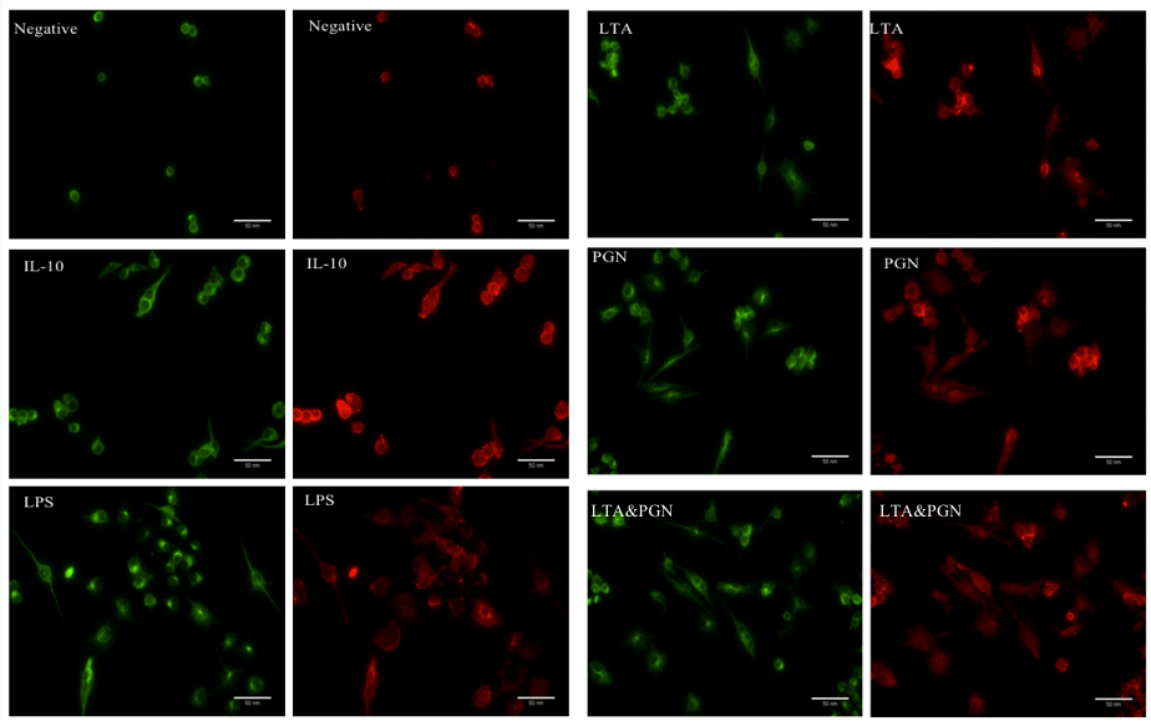

Figure 9: Cell morphology of RAW264.7 macrophages after 18 hours of exposure to *S.aureus* components. Figure shows macrophages at 18 hours of treatment as viewed by immunofluorescence microscopy. Cells were stained for α-β tubulin (green) and phallodin labeled F-actin (red). Scale bars represent 50 μm.

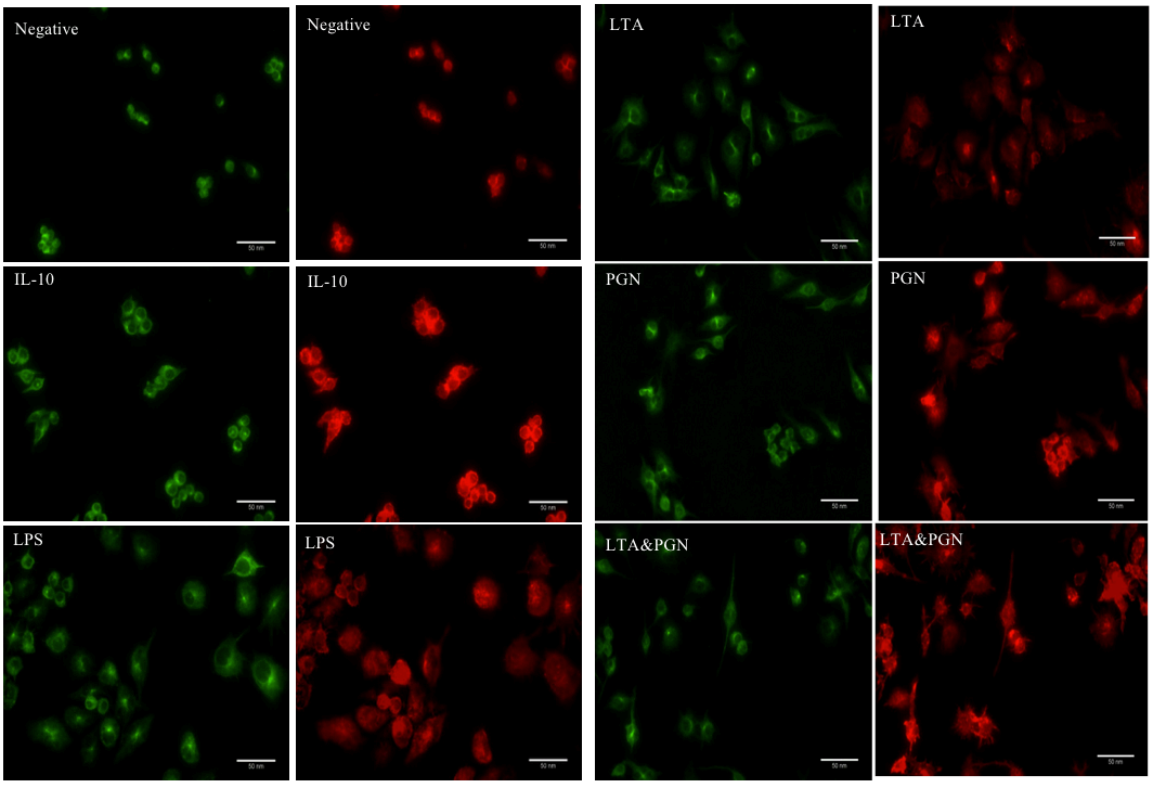

Figure 10: Cell morphology of RAW264.7 macrophages after 24 hours of exposure to *S.aureus* components. Figure shows macrophages at 24 hours of treatment as viewed by immunofluorescence microscopy. Cells were stained for α-β tubulin (green) and phalloidin labeled F-actin (red). Scale bars represent 50 μm.

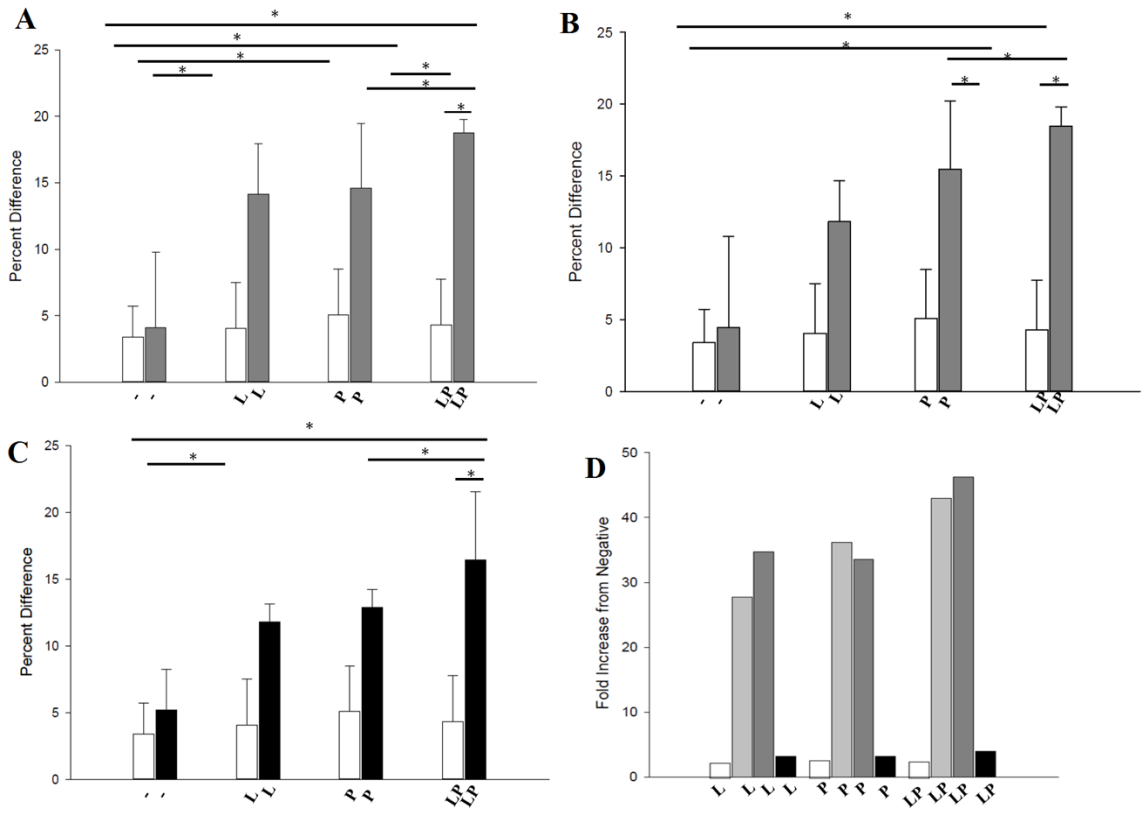

Figure 11: Comparison of intracellular IL-10 production over 24 hours. Figure shows comparison of intracellular IL-10 production between (**A**) 6 and 12 hours of treatment, (**B**) 6 and 18 hours of treatment, (**C**) 6 and 24 hours of treatment. Figure **D** shows mean fold increase from negative control cells in intracellular IL-10 production as observed via flow cytometry. Error bars represent standard error of the mean. (* denotes $P<0.05$) (- = Negative control, LPS= Lipopolysaccharide control, IL-10 = IL-10 control, L= Lipoteichoic acid, P= Peptidoglycan) (white columns denotes treatment at 6 hours, light grey columns denote treatment at 12 hours, dark grey denotes treatment at 18 hours, and black columns denote treatment at 24 hours)

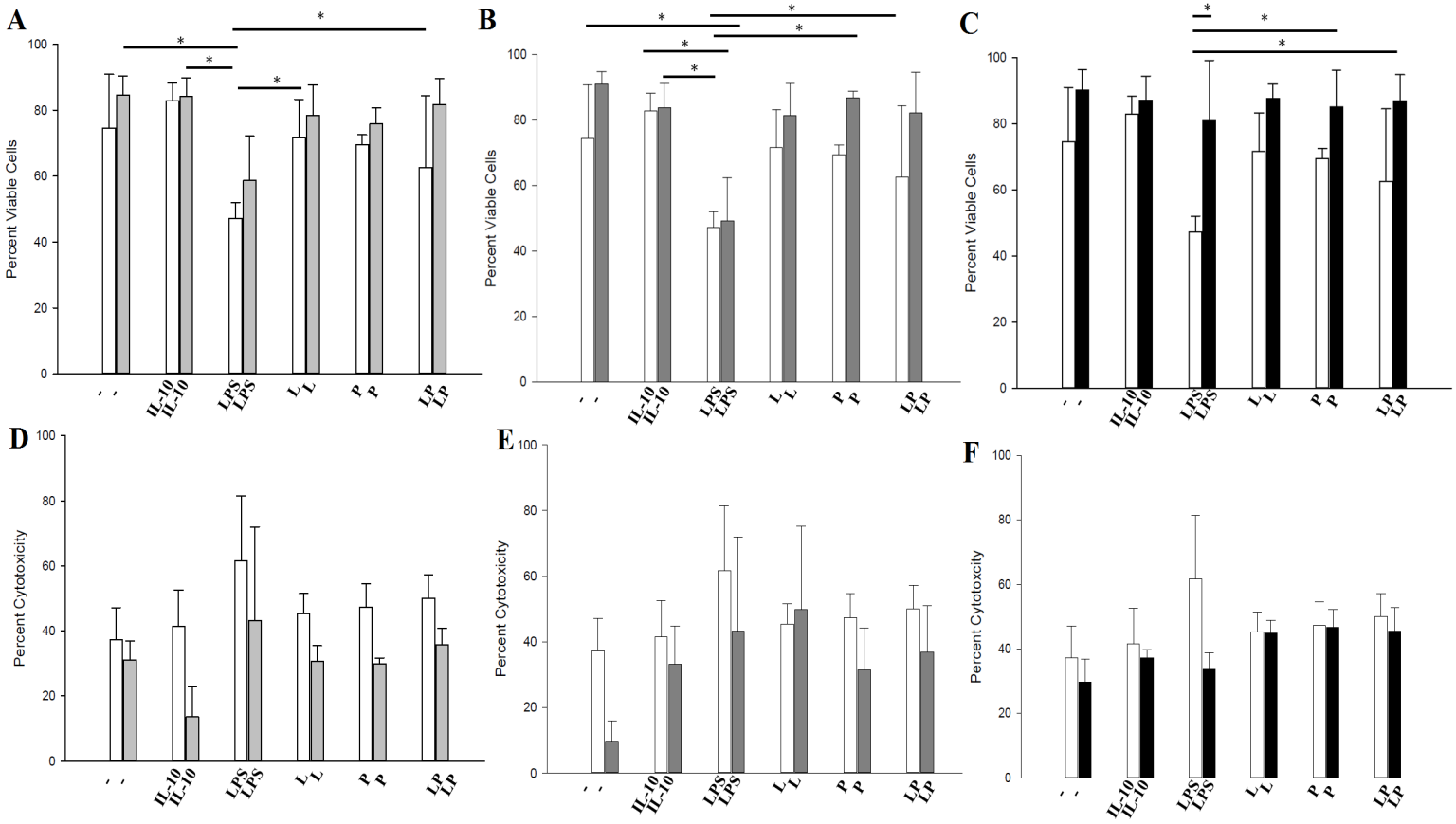

Figure 12: Comparison of cell viability and cytotoxicity in RAW 264.7 macrophages over 24 hours. Figure shows the comparison between cell viability as determined by trypan-blue staining (**A-C**) and cytotoxicity as determined by LDH release (**D-F**) over 24 hours. Comparison between (**A,D**) 6 and 12 hours, (**B,E**) 6 and 18 hours, and (**C,F**) 6 and 24 hours of exposure to *S.aureus* cell wall components. Error bars represent standard error of the mean. (* denotes $P<0.05$) (- =negative control cells, LPS= Lipopolysaccharide positive control, IL-10= IL-10 positive control, L= Lipoteichoic acid, P= Peptidoglycan) (white columns denotes treatment at 6 hours, light grey columns denote treatment at 12 hours, dark grey denotes treatment at 18 hours, and black columns denote treatment at 24 hours)

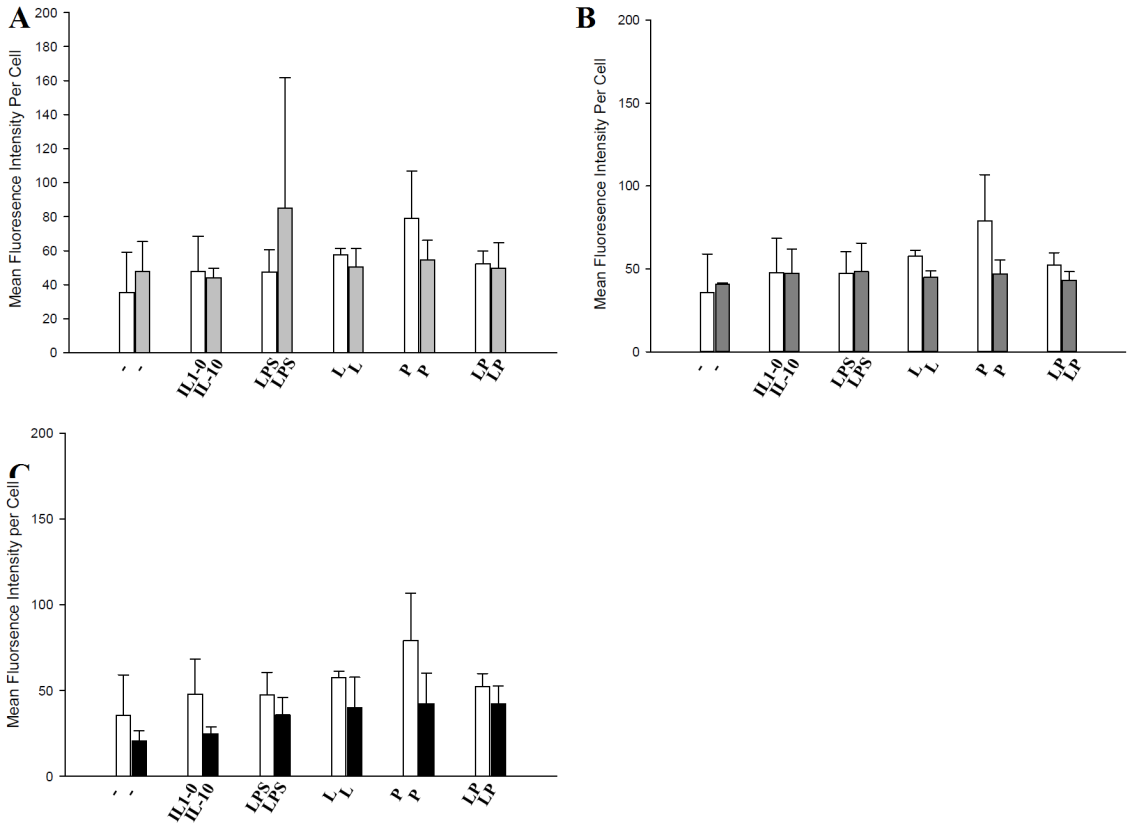

Figure 13: Comparison of α-β tubulin intensity over 24 hours in RAW264.7 macrophages. Figure shows the comparison in α-β tubulin intensity between (**A**) 6 and 12 hours, (**B**) 6 and 18 hours, and (**C**) 6 and 24 hours of exposure to *S.aureus* cell wall components as observed by immunofluorescence microscopy. No significant increase or decrease in α-β tubulin intensity occurred over 24 hours. Error bars represent standard error of the mean. (* denotes $P<0.05$) (- = Negative control, LPS= Lipopolysaccharide control, IL-10 = IL-10 control, L= Lipoteichoic acid, P= Peptidoglycan) (white columns denotes treatment at 6 hours, light grey columns denote treatment at 12 hours, dark grey denotes treatment at 18 hours, and black columns denote treatment at 24 hours)

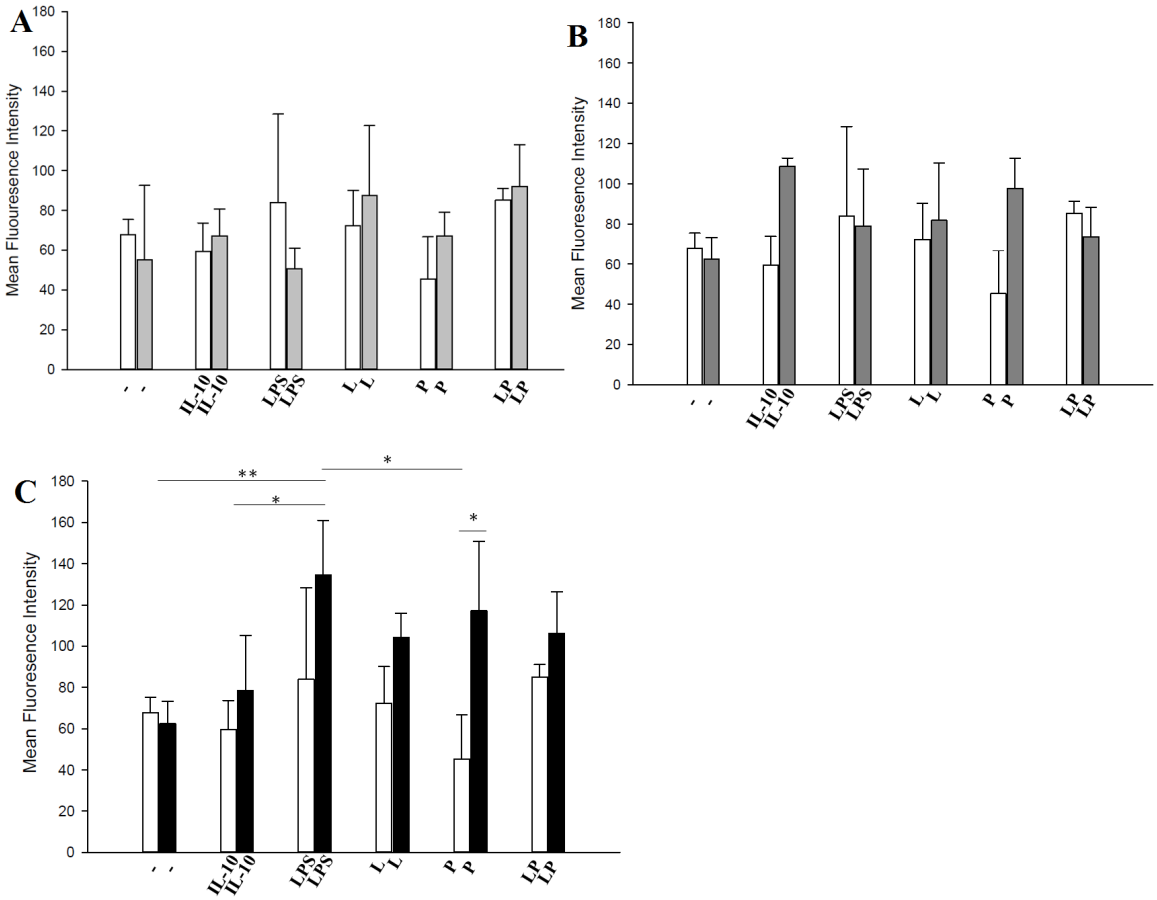

Figure 14: Comparison of phalloidin F-actin intensity over 24 hours in RAW264.7 macrophages. Figure shows the comparison in phalloidin labelled F-actin between (**A**) 6 and 12 hours, (**B**) 6 and 18 hours, and (**C**) 6 and 24 hours of exposure to *S.aureus* cell wall components as observed by immunofluorescence intensity. Error bars represent standard error of the mean. (* denotes $P<0.05$) (- = Negative control, LPS= Lipopolysaccharide control, IL-10 = IL-10 control, L= Lipoteichoic acid, P= Peptidoglycan) (white columns denotes treatment at 6 hours, light grey columns denote treatment at 12 hours, dark grey denotes treatment at 18 hours, and black columns denote treatment at 24 hours)

X. REFERENCES

1. Aulock, S.V., Morath, S., Hareng, L., Knapp, S., Kessel, K.P.M.V., Strijp, J.A.G.V., & Hartung, T., (2003)., **Lipoteichoic acid from *Staphylococcus aureus* is a potent stimulus for neutrophil recruitment**, *Immunobiology*, 208, 413-422
2. Binker, M.G., Zhao, D.Y., Pang, S.J.Y., & Harrison, R.E., (2007), **Cytoplasmic linker protein-170 enhances spreading and phagocytosis in activated macrophages by stabilizing microtubules**, *The Journal of Immunology*, 170, 3780-3791, doi: 10.4049/jimmunolo.179.6.3780
3. Brown, L., Wolf, J.M., Rosalee, R.P., & Casadevall, A., (2015**), Through the wall: extracelular vesicles in gram-positive bacteria, mycobacteria and fungi**, *National Reviews in Microbiology,* 13 (10), 620-630, doi: 10.1038/nrmicro3480
4. David, M.Z., & Daum, R.S., (2010), **Community-associated methicillin-resistant *Staphylococcus aureus*: epidemiology and clinical consequences of an emerging epidemic**, *Clinical Microbiology Reviews*, 23 (3), 616-687, doi: 10.1128/CMR.00081-09
5. Deshmukh, H.S., Hamburger, J.B., Ahn, S.H., McCafferty, D.G., Yang, S.R., & Fowler, V.G.Jr., (2009), **Critical role of NOD2 in regulate the immune response to *Staphylococcus aureus***, *Infection and Immunity*, 77(4), 1376-1382, doi: 10.1128/IAI.00940-08

6. Dominguez, R., & Holmes, K.C., (2011), **Actin structure and function**, *Annual Reviews of Biophysics*, 40, 169-186, doi: 10.1146/annurev-biophys-042910-155359

7. Duque, G.A., & Descoteaux, A., (2014), **Macrophage cytokines: involvement in immunity and infectious diseases**, *Frontiers in Immunology*, 5, 1-12, doi: 10.3389/fimmu.2014.00491

8. Dziarski, R., & Gupta, D., (2005), **Peptidogylcan recognition in innate immunity**, *The Journal of Endotoxin Research*, 11(5), 304-310, doi: 10.1179/096805105X67256

9. Eiff, C.V., Peters, G., & Becker, K., (2006), **The small colony variant (SCV) concept- the role of staphylococcal SCVs in persistent infections**, *Injury: International Journal of the Care of the Injured*, 37, 526-533, doi: 10.1016/j.injury.2006.04.006

10. Foster, T.J., (2005), **Immune evasion by staphylococci**, *Nature Reviews in Microbiology*, 3, 948-958, doi: 10.1038/nrmicro1289

11. Fournier, B., & Philpott, D.J., (2005), **Recognition of *Staphylococcus aureus* by the innate immune system**, *Clinical Microbiology Reviews*, 18(3), 521-540, doi:10.1128/CMR.18.3.521-540.2005

12. Frodermann, V., Chau, T.A., Sayedyahossein, S., Thoth, J.M., Heinrichs, D.E., & Madrenas, J., (2011), **A modulatory interleukin-10 response to staphylococcal**

peptidoglycan prevents Th1/Th17 adaptive immunity to *Staphylococcus aureus*, *Journal of Infectious Disease*, 204, 253-262, doi: 10.1093/infdis/jir276

13. Girardin, S.E., Boneca, I.G., Vinla, J., Chamillard, M., Labigne, A., Thomas, G., Philpott, D.J., & Sansonetti, P.J., (2003), **Nod2 is a general sensor of peptidoglycan through muramyl dipeptide (MDP) detection**, *The Journal of Biological Chemistry*, 278(11), 8869-8872, doi:10.1074/jbc.c200651200

14. Girardin, S.E., Travassos, L.H., Herve, M., Blanot, D., Boneca, I.G., Philpott, D.J., Sansonetti, P.J., & Lexreuix, D.M., (2003), **Peptidoglycan molecular requirements allowing detection by Nod1 and Nod2**, *The Journal of Biological Chemistry*, 278(43), 41702-41708, doi:10.1074/jbc.m307198200

15. Hasko, G., Szabo, C., Nemeth, Z.H., Kvetan, V., Pastores, S.M., & Vizi, E.S., (1996), **Adenosine receptor agonists differentially regulate IL-10, TNF-α, and nitric oxide production in RAW264.7 macrophages and in endotoxemic mice**, *The Journal of Immunology*, 157, 4634-4640

16. Jeon, H., Oh, M.H., Jun, S.O, Kim, S.I., Choi, C.W., Kwon, H.I., Na, S.H., Kim, Y.J., Nicholas, A., Selasi, G.N., & Lee, J.C., (2016), **Variation among *Staphylococcus aureus* membrane vesicle proteomes affects cytotoxicity of host cells**, *Microbial Pathogenesis*, 93, 185-193, doi:10.1016/j.micpath.2016.02.014

17. Jiang, S., Ghoshdastider, U., Narita, A., Popp., D., & Robinson, R.C., (2006), **Structural complexity of filaments form from the actin and tubulin folds**,

Communicative and integrative biology, 9(6), 1-6, doi:10.1080/19420889.2016.1242538

18. Lin, Y.C., Peterson, M.L., (2010), **New insights into the prevention of staphylococcal infections and toxic shock syndrome**, *Expert Review in Clinical Pharmacology*, 3(6), 753-767, doi: 10.1586/exp.10.121

19. Lumeng, C.N., Bodzin, J., Saltiel, A.R., (2007), **Obesity induces a phenotypic switch in adipose tissue macrophage polarization**, *The Journal of Clinical Investigation*, 117(1), 176-184, doi:10.1172/JCI29881

20. McWhorter, F.Y., Wang, T., Nguyen, P., Chung, T., & Liu, W.F., (2013), **Modulation of macrophage phenotype by cell shape**, *PNAS*, 110(43), 17253-17258, doi:10.1073/pnas.1308887110

21. Miller, L.S., Cho, J.S., (2011), **Immunity against *Staphylococcus aureus* cutaneous infections**, *Nature Reviews Immunology*, 11, 505-518, doi: 10.1038/nri3010

22. Morath, s., Geyer, A., Spreitzer, I., Hermann, C., & Hartung, T., (2002), **Structural decomposition and heterogeneity of commercial lipoteichoic acid preparations**, *Infection and Immunity*, 70(2), 938-944, doi:10.1128/IAI.70.2.938-944.202

23. Murray, R.Z., Wylie, F.G., Khromykh, T., Hume, D.A., & Stow, J.L., (2005), **Syntaxin 6 and Vti1b form a novel SNARE complex which is up-regulated in activated macrophages to facilitate exocytosis of tumor necrosis factor-α**, *The*

Journal of Biological Chemistry, 280(11), 10478-10483, doi:10.1074/jbx.M414420200

24. Naimi, T.S., LeDell., K.H., Sabetti, K.C., Borchardt, S.M., Boxrud, D.J., Etienne, J., Johnson, S.K., Vandenesch, F., Fridkin, S., O'Boyle, C., Danila, R.N., & Lynfield, R., (2003), **Comparison of community- and health care-associated methicillin-resistant *Staphylococcus aureus* infection**, *Journal of the American Medical Association*, 290(22), 2976-2984

25. Otto, M., (2014), ***Staphylococcus aureus* toxins**, *Current Opinion in Microbiology*, (0), 32-37, doi:10.1016/j.mib.2013.11.004

26. Pengal, R.A., Ganesan, L.P., Wei, G., Fang, H., Ostrowski, M.C., & Tridanadpani, S., (2006), **Lipopolysaccharide-induced production of interleukin-10 is promoted by the serine/threonine kinase Akt**, *Molecular Immunology*, 43, 1557-1564, doi:10.1016/j.molimm.2005.09.022

27. Ratner, A.J., Aguilar, J.L., Shchepetov, M., Lysenko, E.S., & Weiser, J.N., (2007), **Nod1 mediates cytoplasmic sensing of combinations of extracellular bacteria**, *Cell Microbiology*, 9(5), 1343-1351

28. Robinson, J.M., & Vandre, D.D., (1995), **Stimulus-dependent alterations in macrophage microtubules: increased tubulin polymerization and detyrosination**, *Journal of Cell Science*, 106, 645-655

29. Saravia, M., & O'Garra, S., (2010), **The regulation of IL-10 production by immune cells**, *Nature Reviews*, 10, 170-182, doi:10.1038/nri2711

30. Schroder, N.W.J., Morath, S., Alexander, C., Hamann, L., Hartung, T., Zahringer, U., Gobel, U.B., Weber, J.R., & Schumann, R.R., (2003), **Lipoteichoic acid (LTA) of *Streptococcus pneumoniae* and *Staphylococcus aureus* activates immune cells via toll-like receptor (TLR)-2, lipopolysaccharide-binding protein (LBP), and CD14, whereas TLR-4 and MD-2 are not involved**, *The Journal of Biological Chemistry*, 278(18), 15587-15594, doi:10.1074/jbc.M212829200

31. Shinefeild, H.R., & Ruff, N.L, (2009), **Staphylococcal infections: a historical perspective**, *Infectious Disease Clinics of North America*, 23(1), 1-15, doi:10.1016/j.idc.2008.10.007

32. Shinohara, H., Behar, N., Inoue, K., Hiroshima, M., Yasuda, T., Nagashima, T., Kimura, S., Sanjo, H., Maeda, S., Yumoto, N., Ki, S., Sako, Y., Hoffmann, A., Kurosaki,T., & Hatakeyama, M.O., (2014), **Positive feedback within a kinase signaling complex functions as a switch mechanism for NF-κB activation**, *SCIENCE*, 344, 760-766, doi:10.1126/science.1250020

33. Sullivan, K.E., Reddy, A.B.M., Dietzmann, K., Suriano, A.R., Kocieda, V.P., Stewart, R., & Bhatia, M., (2007), **Epigenetic regulation of tumor necrosis factor-α**, *Molecular and Cellular Biology*, 27(14), 5147-5160, doi:10.1128/MCB.02429-06

34. Thammavongsa, V., Missiaka, D.M., Schneewind, O., (2013), ***Staphylococcus aureus* degrades neutrophil extracellular traps to promote immune cell death**, *Science*, 15, 863-866, doi:10.1126/science.124455

35. Valeva, A., Walev, I., Pinkernell, M., Walker, B., Bayley, H., Pamer, M., & Bhakdi, S., (1997), **Transmembrane beta-barrel of staphylococcal α-toxin forms in sensitive but not resistant cells**, *Proceedings of the National Academy of Science*, 94, 11607-11611

36. Ventola, C.L., (2015), **The antibiotic resistance crisis**, *Pharmacy and Therapeutics*, 40(4), 277-283

37. Vereyken, E.J.F., Heijnen, P.D.A.M., Varon, W., Vires, E.H.E.D., Dijkstra, C.D., & Teunissen, C.E., (2011), **Classically and alternatively activated bone marrow derived macrophages differ in cytoskeletal functions and migration towards specific CNS cell types**, *Journal of Neuroinflammation*, 8, 58-74

38. Verma, R., Balakrishnan, L., Sharma, K., Khan, A.A., Advani, J., Gowda, H., Tripathy, S.P., Suar, M., Pandey, A., Ganotra, S., Prasad, T.SK., & Shankar, S., (2016), **A network map of interleukin-10 signaling pathway**, *Journal of Cell Communication Signaling*, 10, 61-67, doi:10.1007/s12079-015-0303-x

39. Warenburg, J.B., Williams, W.A., & Missiakas, D., (2006), **Host defenses against *Staphylococcus aureus* infection require recognition of bacterial lipoproteins**, *PNAS*, 103(37), 13831-13836, doi:10.1073/pnas.0603072103

40. Wu, X., and Wu, F., (2014), **Dendritic cells during *Staphlyococcus aureus* infection: subtypes and roles**, *Journal of Translational Medicine*, 12, 358-367

XI. Appendix

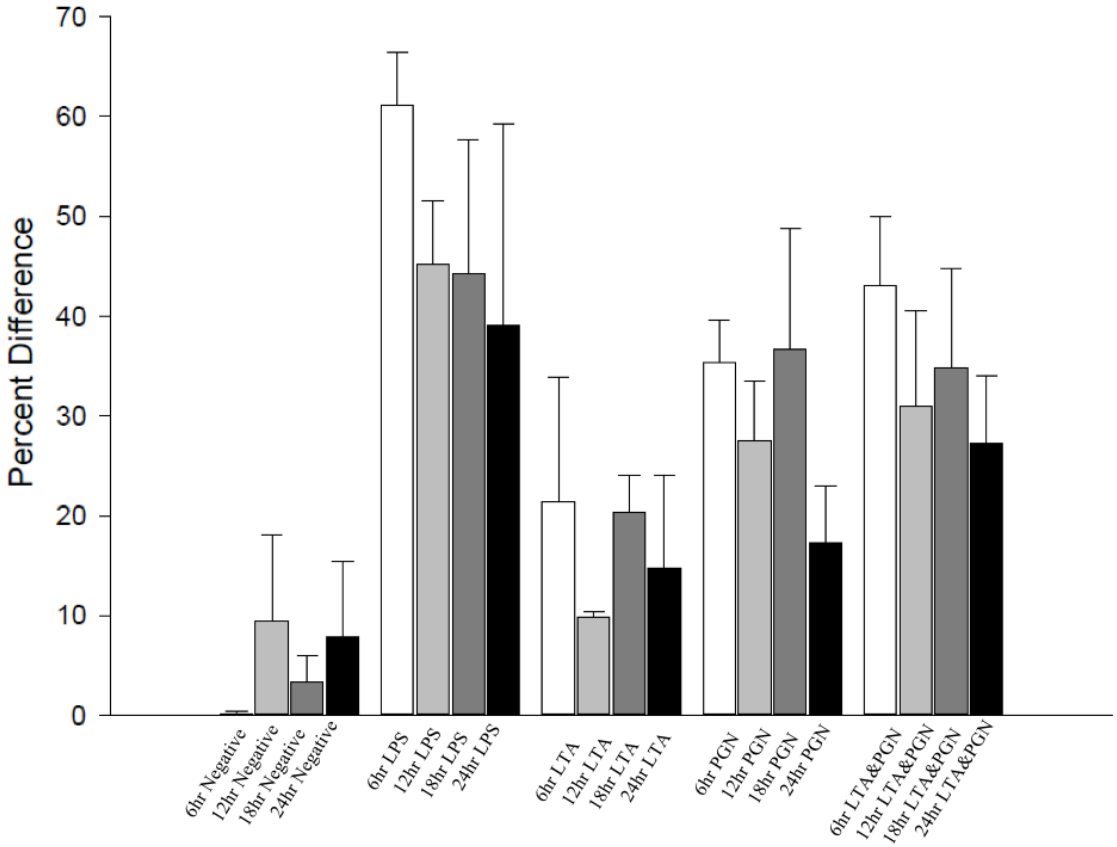

Appendix Figure 1: Cumulative intracellular TNF-α production in RAW264.7 macrophages over 24 hours. Figure shows the trend in intracellular TNF-α production over 24 hours. Intracellular cytokines were assessed by flow cytometry after each experimental time period. Error bars represent standard error of the mean.

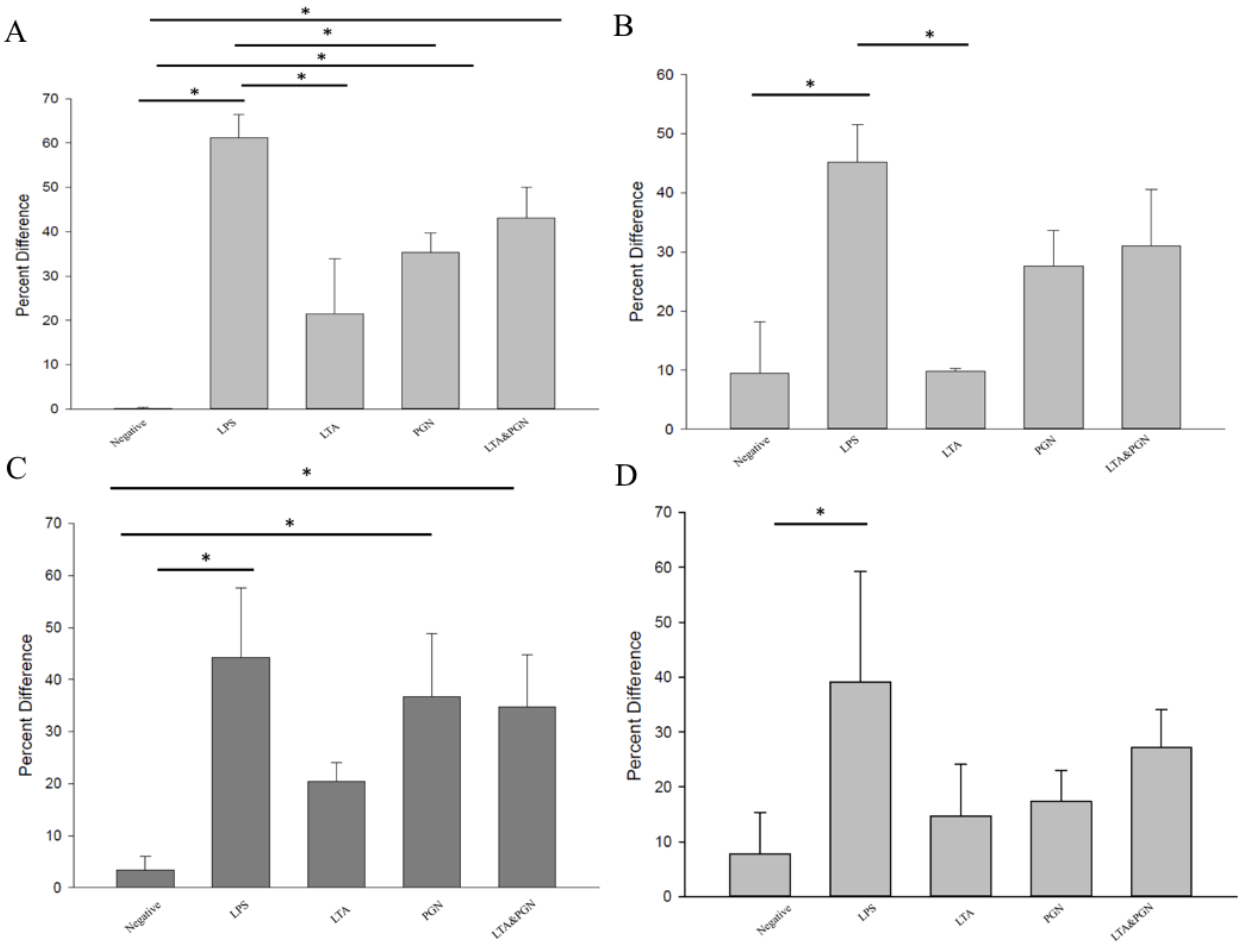

Appendix Figure 2: Intracellular TNF-α production in RAW264.7 macrophages from 6 to 24 hours. Figure shows the intracellular TNF-α production at (**A**) 6, (**B**) 12, (**C**) 18, and (**D**) 24 hours of exposure to *S.aureus* cell wall components as assessed by Flow Cytometry. Error bars represent standard error of the mean. (* denotes P<0.05)

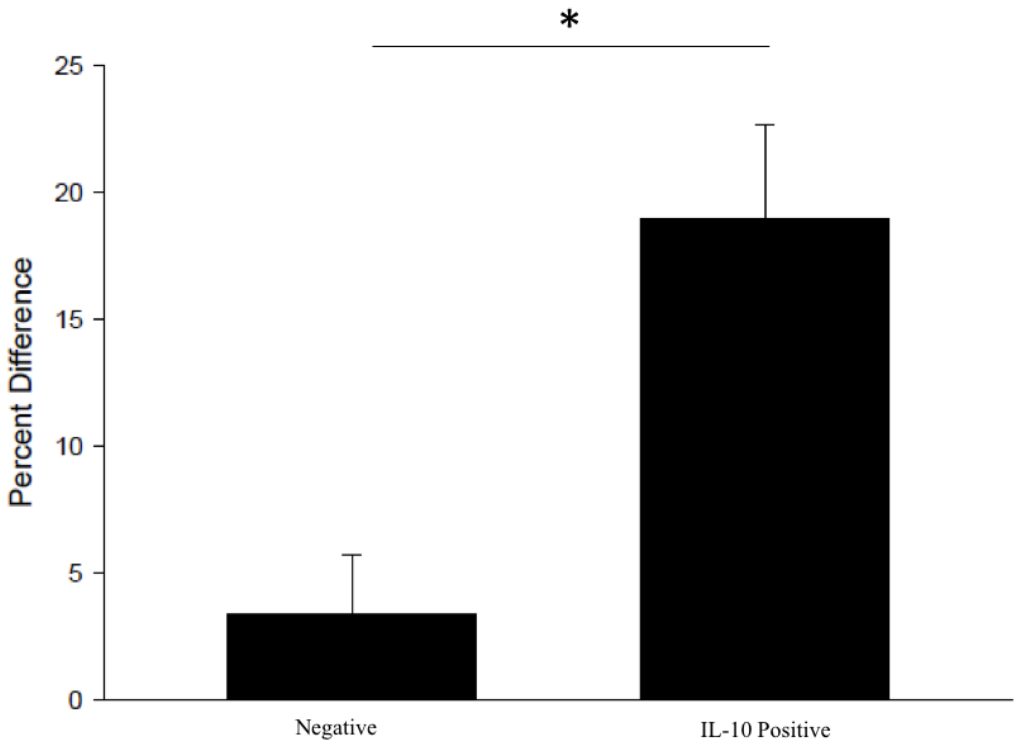

Appendix Figure 3: IL-10 positive control cytokine production. Figure shows IL-10 production after treatment with 100 ng/mL of IL-10 as determined by flow cytometry. Positive control was used to determine antibody specificity. Error bars represent standard error of the mean. (* denotes $P<0.05$)

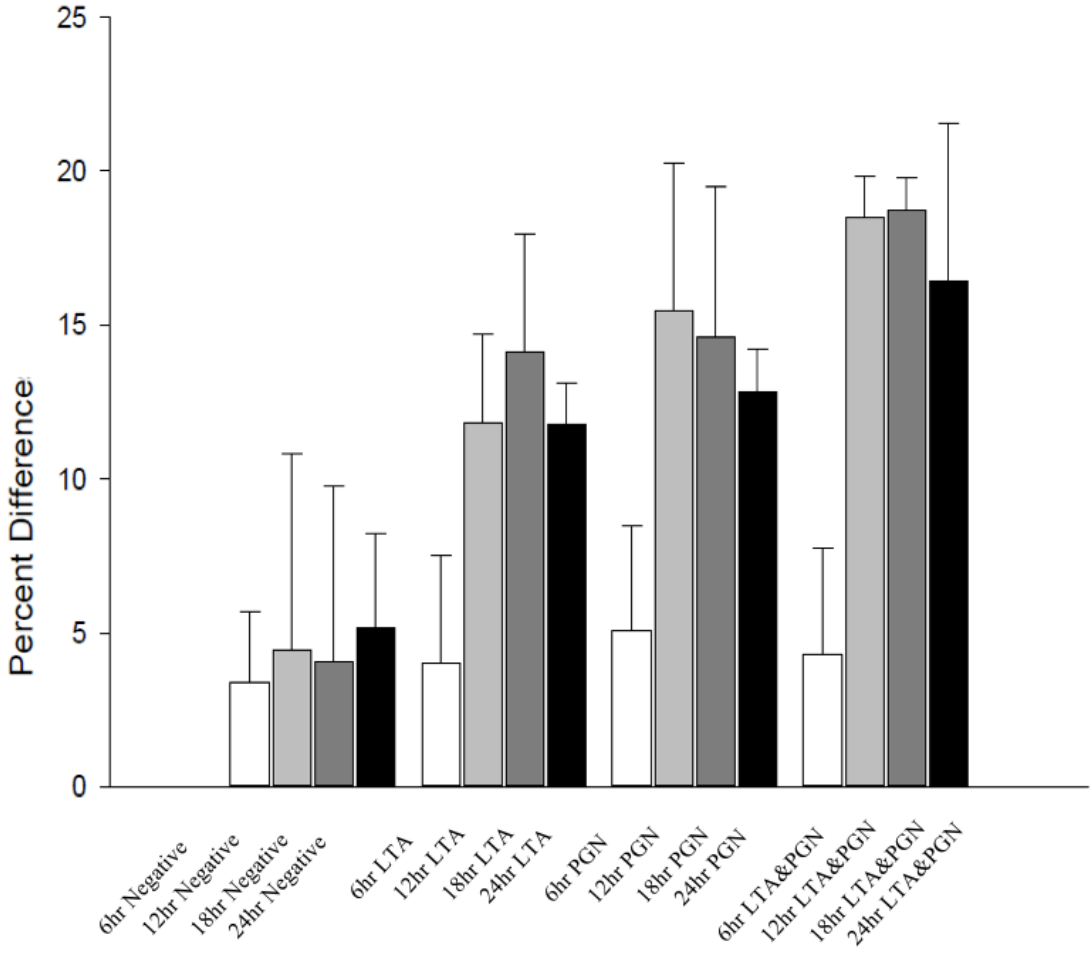

Appendix Figure 4: IL-10 Cytokine production by RAW264.7 macrophages over 24 hours. RAW264.7 cells were treated with *S.aureus* cell wall components LTA, PGN, and combination of LTA and PGN over twenty four hours. Intracellular cytokines were measured by Flow Cytometry after each experimental trial period. Figure shows overall trend of IL-10 production. Error bars represent standard error of the mean.

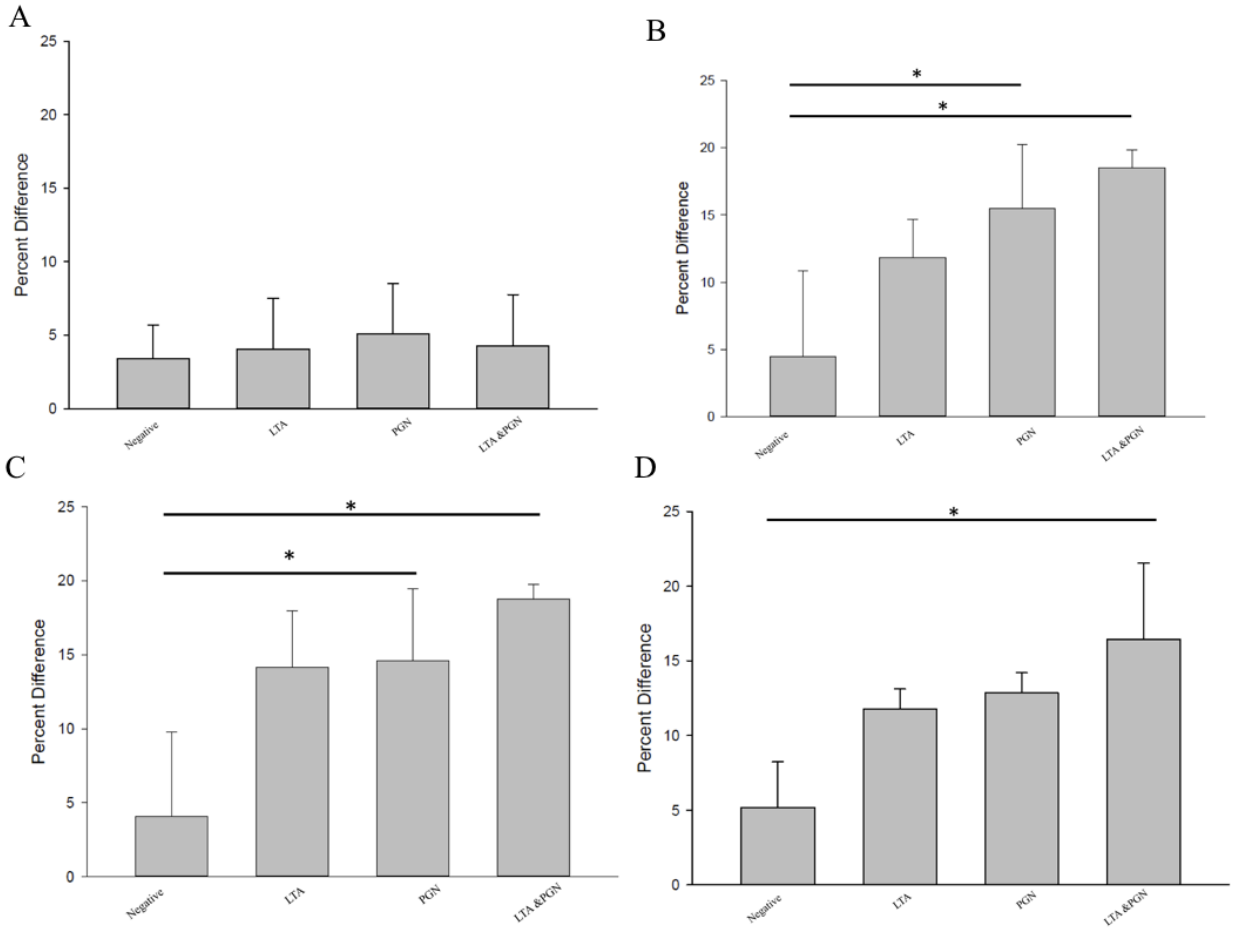

Appendix Figure 5: Intracellular IL-10 Cytokine Production in RAW264.7 macrophages from 6 to 24 hours. Figure shows intracellular IL-10 cytokines as assessed at (**A**) 6, (**B**) 12, (**C**)18, and (**D**) 24 hours via flow cytometry. Error bars represent standard error of the mean. (* denotes $P<0.05$)

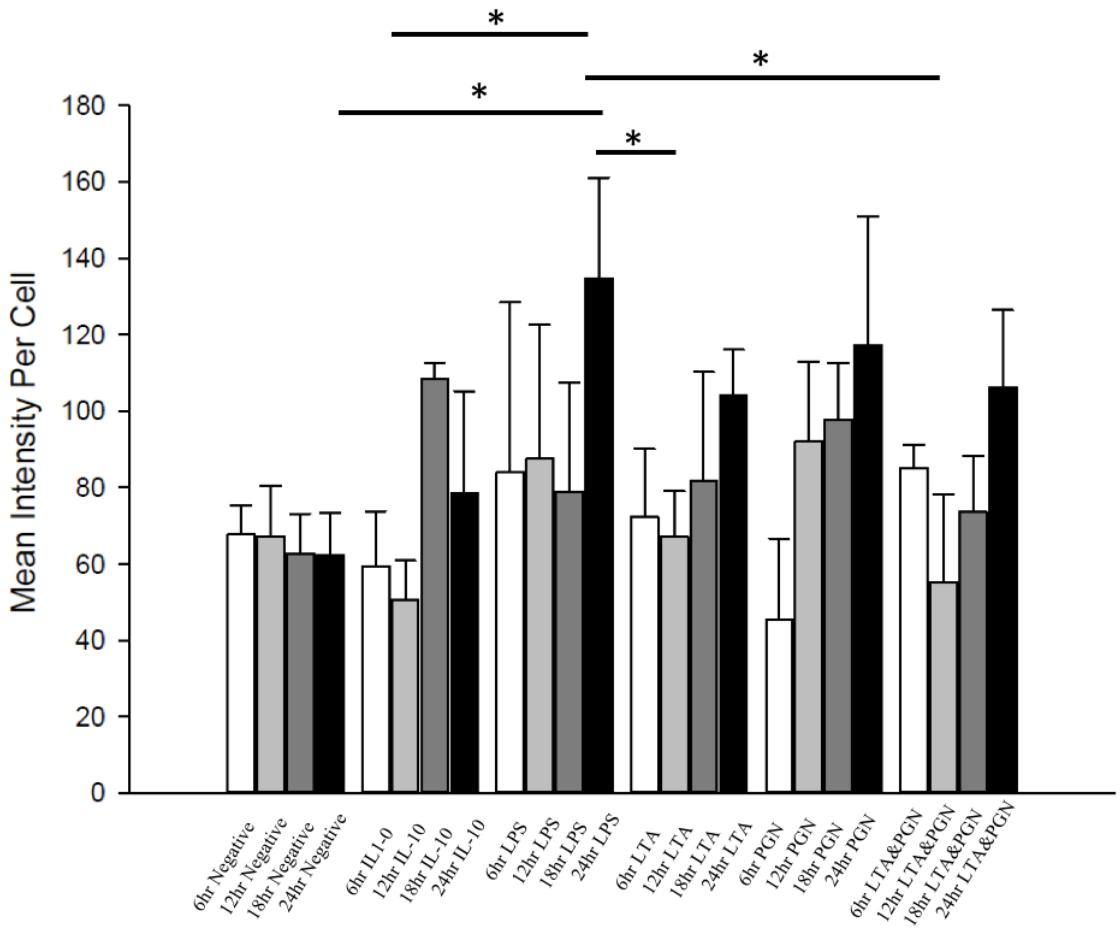

Appendix Figure 6: Cumulative F-Actin Intensity in RAW264.7 macrophages after treatment of *S.aureus* components over 24 hours. Figure shows the mean F-actin fluorescence intensity per cell as observed by immunofluorescence microscopy over 24 hours. Error bars represent standard error of the mean. (* denotes $P<0.05$)

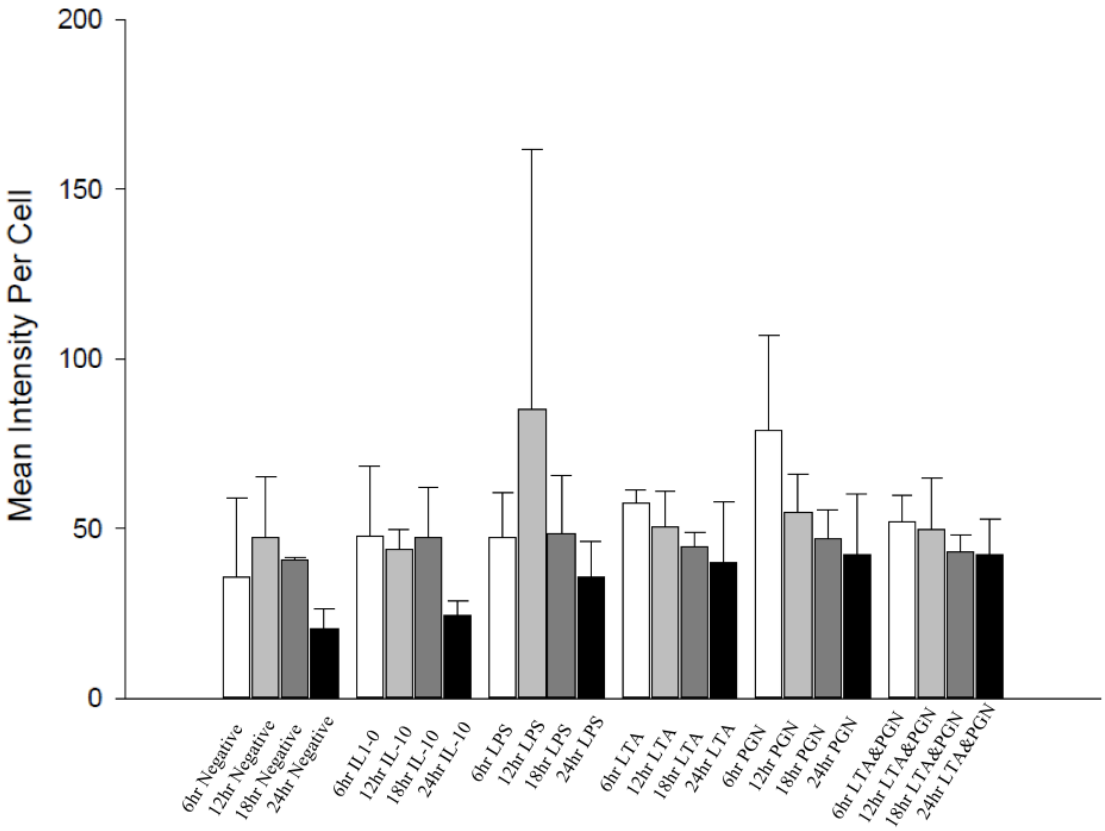

Appendix Figure 7: Cumulative α-β Tubulin Intensity in RAW264.7 macrophages after treatment of *S.aureus* components over 24 hours. Figure shows mean α-β tubulin intensity per cell over 24 hours as observed by immunofluorescence microscopy. Error bars represent standard error of the mean.

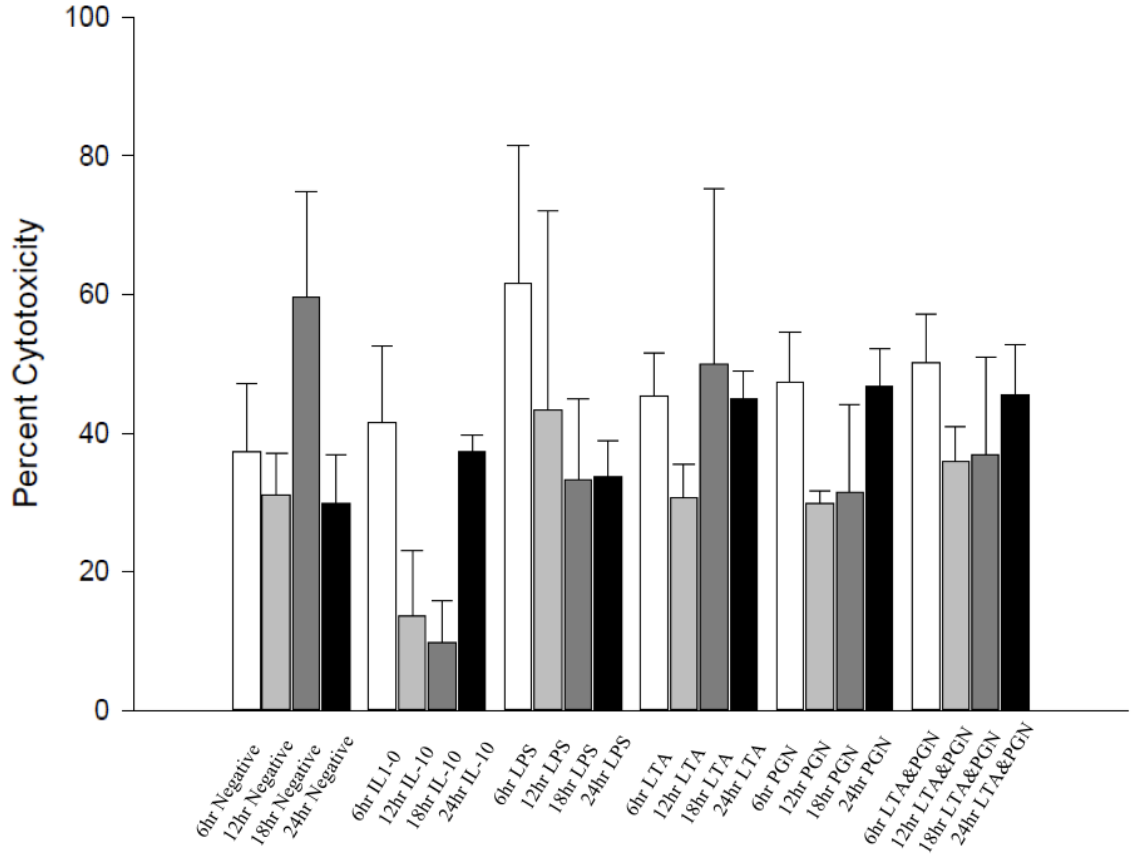

Appendix Figure 8: Cumulative Cytotoxicity in RAW264.7 macrophages after treatment with *S.aureus* components over 24 hours. Figure shows cytotoxicity in macrophages after treatment with *S.aureus* cell wall components as observed by a LDH assay. No significant increase in cytotoxicity occurred when cells were treated with *S.aureus* cell wall components. Error bars represent standard error of the mean.

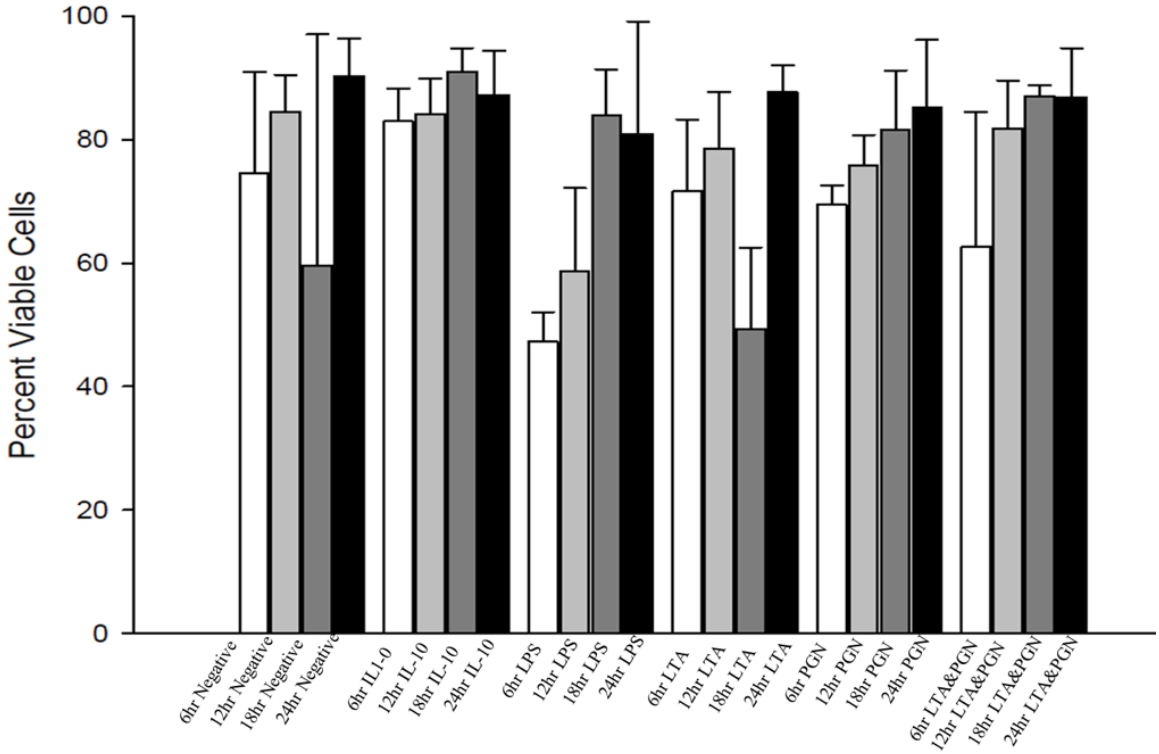

Appendix Figure 9: Cumulative cell viability in RAW264.7 macrophages after treatment with *S.aureus* components over 24 hours. Figure shows macrophage cell viability over 24 hours as observed by trypan-blue staining. No significant decrease in cell viability occurred when cells were treated with *S.aureus* cell wall components. Error bars represent standard error of the mean.